

Chemical speciation models based upon the Pitzer activity coefficient equations, including the propagation of uncertainties. II. Tris buffers in artificial seawater at 25 °C, and an assessment of the seawater ‘Total’ pH scale

Simon L. Clegg^{a,*}, Matthew P. Humphreys^{a,b}, Jason F. Waters^c, David R. Turner^d, Andrew G. Dickson^e

^a School of Environmental Sciences, University of East Anglia, Norwich NR4 7TJ, United Kingdom

^b NIOZ Royal Netherlands Institute for Sea Research, Department of Ocean Systems (OCS), P.O. Box 59, 1790 AB Den Burg, Texel, The Netherlands

^c National Institute of Standards and Technology, Gaithersburg, MD 20899, USA

^d Department of Marine Sciences, University of Gothenburg, Box 461, SE-40530 Gothenburg, Sweden

^e University of California at San Diego, Scripps Institution of Oceanography, 9500 Gilman Drive, La Jolla, CA 92093, USA

ARTICLE INFO

Keywords:

Seawater

Total pH

Chemical speciation

Tris buffer

Activity coefficient

Pitzer model

ABSTRACT

The substance Tris (or THAM, 2-amino-2-hydroxymethyl-1,3-propanediol, CAS 77–86-1), and its protonated form TrisH^+ , is used in the preparation of pH buffer solutions for applications in seawater chemistry. The development of an acid-base chemical speciation model of buffer solutions containing Tris, TrisH^+ , and the major ions of seawater is desirable so that: (i) the effects of changes in the composition of the medium on pH can be calculated; (ii) pH on the free (a measure of $[\text{H}^+]$) and total (a measure of $([\text{H}^+] + [\text{HSO}_4^-])$) scales can be interconverted; (iii) approximations inherent in the definition of the total pH scale can be quantified; (iv) electrode pairs such as H^+/Cl^- and H^+/Na^+ can more easily be calibrated for the measurement of pH. As a first step towards these goals we have extended the Pitzer-based speciation model of Waters and Millero (Mar. Chem. 149, 8–22, 2013) for artificial seawater to include Tris and TrisH^+ , at 25 °C. Estimates of the variances and covariances of the additional interaction parameters were obtained by Monte Carlo simulation. This enables the total uncertainty of any model-calculated quantity (e.g., pH, speciation) to be estimated, as well as the individual contributions of all interaction parameters and equilibrium constants. This is important for model development, because it allows the key interactions to be identified. The model was tested against measured EMFs of cells containing Tris buffer in artificial seawater at 25 °C, and the mean deviation was found to be 0.13 ± 0.070 mV for salinities 20 to 40. Total variances for calculated electromotive forces of the buffer solutions are dominated by contributions from just a few interaction parameters, making it likely that the model can readily be improved. The model was used to quantify the difference between various definitions of total pH and $-\log_{10}([\text{H}^+] + [\text{HSO}_4^-])$ in Tris buffer solutions at 25 °C, for the first time (item (iii) above). The results suggest that the total pH scale can readily be extended to low salinities using the established approach for substituting TrisH^+ for Na^+ in the buffer solutions, especially if the speciation model is used to quantify the effect on pH of the substitution. The relationships between electromotive force (EMF), and pH on the total scale, with buffer molality in artificial seawater at constant salinity are shown to be linear above about 0.01 to 0.02 mol kg^{-1} buffer molality. The pH of Tris buffers containing ratios of TrisH^+ to Tris that vary from unity can be calculated very simply. Technical aspects of the total pH scale, such as the extrapolation of pH to zero buffer (at constant salinity), are clarified. Recommendations are made for further work to extend the model to the temperature range 0–45 °C, and improve accuracy, so that requirements (i) to (iv) above can be fully met.

* Corresponding author.

E-mail address: s.clegg@uea.ac.uk (S.L. Clegg).

<https://doi.org/10.1016/j.marchem.2022.104096>

Received 17 August 2021; Received in revised form 2 February 2022; Accepted 3 February 2022

Available online 8 February 2022

0304-4203/© 2022 The Authors. Published by Elsevier B.V. This is an open access article under the CC BY license (<http://creativecommons.org/licenses/by/4.0/>).

Glossary of symbols

Pitzer interaction parameters

$\beta_{ca}^{(0)}$, $\beta_{ca}^{(1)}$, $\beta_{ca}^{(2)}$, $C_{ca}^{(0)}$, $C_{ca}^{(1)}$ For interactions between cation c and anion a. Not all of these may be used, e.g., $\beta_{ca}^{(2)}$ is usually for 2:2 charge types only (e.g., CaSO_4), and is set to zero otherwise.

α_{ca} , $\alpha_{ca}^{(2)}$, ω_{ca} Coefficients associated with the ionic strength terms in the functions that use parameters $\beta_{ca}^{(1)}$, $\beta_{ca}^{(2)}$, and $C_{ca}^{(1)}$, respectively.

θ_{cc} , θ_{aa} For interactions between dissimilar cations c and c', and between dissimilar anions a and a', respectively.

$\psi_{cc'a}$, $\psi_{aa'c}$ For interactions between anion a and dissimilar cations c and c', and between cation c and dissimilar anions a and a', respectively.

λ_{nc} , λ_{na} For interactions between neutral solute n and cation c, and between neutral solute n and anion a, respectively.

λ_{nn} , μ_{nnn} For the self-interaction of neutral solute n.

ζ_{nca} For interaction between neutral solute n, cation c and anion a.

Other symbols used in the text

a_X Activity (molality basis) of species X, equivalent to $m_X \cdot \gamma_X$ where γ_X is the activity coefficient of X.

C_p Heat capacity of an aqueous solution, at constant pressure.

E Electrode potential (V) in a Harned cell.

E^0 Standard electrode potential (V) of a Harned cell.

E^* The standard potential (V), on a total H^+ basis, defined by Eq. (12), and obtained by extrapolating Harned cell potentials to zero HCl molality in an artificial seawater of a specified composition (nominal salinity).

$E_{R(1)}$, $E_{R(2)}$ Electrode potentials (V) in Harned cells with $\text{TrisH}^+:\text{Tris}$ buffer ratios R(1) and R(2) respectively.

δE The deviation (V) of measured EMFs from the mean of $[E + (RT/F) \cdot \ln(m\text{TrisH}^+/m\text{Tris})]$ for three ratios of buffer. This quantity is used in Fig. 7, and is a measure of how the experimental EMFs differ from the simple empirical relationship described in Section 5.4.

ΔE The activity coefficient contribution to the difference in EMF between a solution (at fixed salinity and temperature) containing molalities m of equimolar Tris and TrisH^+ , and one containing zero buffer. (See Eq. (7) and Table 6.)

ΔE^* The difference in E^* that arises from the use of values obtained for pure artificial seawater for solutions that also contain Tris buffer. See Eq. (14).

F The Faraday constant ($96,485.33212 \text{ C mol}^{-1}$).

I Ionic strength, on a molality basis ($0.5 \sum_i m_i |z_i|^2$, where z_i is the charge on ion i and the summation is over all ions).

K Thermodynamic equilibrium constant (molality basis), expressing the relationship between the quotient of the activities of the product(s) and reactant(s). It is a function of temperature and pressure. Example: $K(\text{TrisH}^+) = a\text{H}^+ \cdot a\text{Tris} / a\text{TrisH}^+$, where a denotes activity.

K^* Stoichiometric equilibrium constant (on a molality basis), expressing the relationship between the quotient of the molalities of the product(s) and reactant(s). It varies with temperature, pressure, and solution composition. Example: $K^*(\text{TrisH}^+) = m\text{H}^+ \cdot m\text{Tris} / m\text{TrisH}^+$, which is equal to $K(\text{TrisH}^+) \cdot \gamma_{\text{TrisH}} / (\gamma_{\text{H}} \cdot \gamma_{\text{Tris}})$.

$K^*(\text{HSO}_4^-)^{(\text{tr})}$ Trace value of the stoichiometric bisulphate dissociation constant in artificial seawater (mol kg^{-1}). See the Appendix concerning the meaning of *trace*, and Eq. (10) for the expression for $K^*(\text{HSO}_4^-)$.

m_X Molality of species X (moles per kg of pure water solvent, with the units “ mol kg^{-1} ”).

$m\text{H}^{+(\text{T})}$ The operational total hydrogen ion molality obtained from a measurement of pH on the total scale (which is calibrated from Harned cell measurements, and incorporates the assumption that the activity coefficient of HCl is independent of the presence of the Tris buffer). Note: $-\log_{10}(m\text{H}^{+(\text{T})}) = \text{pH}_{\text{T},m}$.

$(m\text{H}^{+(\text{T})})_f$ The formal total hydrogen ion molality, as defined by Dickson (1990) and DelValls and Dickson (1998), which is related to the formal total pH by $-\log_{10}[(m\text{H}^{+(\text{T})})_f] = (\text{pH}_{\text{T},m})_f$. The operational and formal total hydrogen ion molalities (and corresponding pH) are the same in artificial seawater and seawater media, but differ in Tris buffer solutions.

$m\text{H}^+ + m\text{HSO}_4^-$ The conventional thermodynamic total hydrogen ion molality (the sum of the conventional thermodynamic H^+ and HSO_4^- molalities in an aqueous solution).

$m\text{SO}_4^{2-(\text{T})}$ Total molality of sulphate in an aqueous solution.

$\text{pH}_{\text{F},m}$ pH on the free scale (on a molality basis), which is defined in box (4) of Chart 1.

$\text{pH}_{\text{F},m}^*$ The quantity $-\log_{10}(m\text{H}^+)$, where $m\text{H}^+$ is the conventional thermodynamic free H^+ molality. The value of $\text{pH}_{\text{F},m}^*$ is related to $\text{pH}_{\text{T},m}^*$ by the equation given in box (2) of Chart 1.

$\text{pH}_{\text{T},m}$ Operational pH on the total scale, and on a molality basis, as defined by DelValls and Dickson (1998). See box (3) of Chart 1.

$\text{pH}_{\text{T},m}^*$ The quantity $-\log_{10}(m\text{H}^+ + m\text{HSO}_4^-)$, where $m\text{H}^+$ and $m\text{HSO}_4^-$ are the conventional thermodynamic H^+ and HSO_4^- molalities. The value of $\text{pH}_{\text{T},m}^*$ is related to $\text{pH}_{\text{T},m}$ by the equation given in box (3) of Chart 1.

$(\text{pH}_{\text{T},m})_f$ The formal total pH on molality basis, see box (5) of Chart 1.

$\text{p}K$ $-\log_{10}$ (of a thermodynamic equilibrium constant, K).

$\text{p}K^*$ as above, but for the stoichiometric equilibrium constant K^* .

$\text{p}X$ The vapour pressure of species X.

R The gas constant ($8.31446 \text{ J mol}^{-1} \text{ K}^{-1}$).

S Salinity. Strictly, any formal definition refers to a natural seawater only. For the artificial seawaters in this work S is a nominal salinity.

T Temperature (K).

γ_X Activity coefficient of species X, on a molality basis.

$\gamma_{\text{HCl}}^{(\text{tr})}$ Trace value of the mean activity coefficient of HCl. See the Appendix concerning the meaning of the word *trace*.

ν_+ (or ν_c), ν_- (or ν_a) Stoichiometric numbers for the cation and anion, respectively, in a salt.

σ Standard uncertainty of a measured or predicted property.

ϕ Molal osmotic coefficient of a solution.

ϕ_E Pseudo-experimental osmotic coefficient, used in re-evaluation of the Pitzer interaction parameters for TrisHCl .

1. Introduction

The seawater total hydrogen ion pH scale (pH being a measure of $-\log_{10}([\text{H}^+] + [\text{HSO}_4^-])$, where the brackets indicate quantities expressed in moles per kg of solution) was established by [DelValls and Dickson \(1998\)](#) from measurements of the EMFs of solutions containing equimolar Tris and its conjugate acid TrisH^+ in artificial seawater, over the temperature range 0 to 45 °C and for salinities from 20 to 40. Measurements that yield the standard EMF, E^* , which are essential to calculations of the total pH, have been made over the larger salinity range of 5 to 45 and for the same temperatures ([Dickson, 1990](#)). [Mosley et al. \(2004\)](#) estimated the pH of Tris buffer solutions at low salinities and 25 °C by interpolating between the data of [DelValls and Dickson \(1998\)](#) and results of [Bates and Hetzer \(1961\)](#) for solution ionic strengths up to 0.1 mol kg⁻¹. [Müller et al. \(2018\)](#) and [Müller and Rehder \(2018\)](#) have attempted to extend the total pH scale from salinity 20 to salinity 5 (and from 5 to 45 °C) using similar methods to [Dickson \(1990\)](#) and [DelValls and Dickson \(1998\)](#). However, the compositions of the solutions measured by Müller et al. and Müller and Rehder were such that they do not extrapolate to that of artificial seawater in the limit of zero added HCl or Tris buffer, and this introduces biases of the order of -0.005 to -0.01 units in the defined total pH for this limiting composition ([Clegg, pers. comm.](#)).

The calibration of total pH, together with its measurement, remain problematic below salinity 20 for the reason given above. Furthermore, the seawater total pH scale applies only to saline waters containing the major ions of seawater approximating the ratios found in the open ocean. A chemical speciation model of Tris buffers in artificial seawater and related saline media, yielding concentrations and activities of H^+ , HSO_4^- , TrisH^+ , Tris and other species, can potentially assist us to clarify these and other issues related to seawater pH:

- A model is needed to extend the total pH scale to low salinity waters, for which Tris and TrisH^+ make up an increasing proportion of the total solutes in the buffer solution as salinity is reduced, thus changing the acid-base properties of the solution by more than is the case for buffers at higher (seawater) salinities.
- A speciation model can potentially be used to calculate the pH of buffers, on different scales, for saline waters whose stoichiometry (i. e., the ratios of the concentrations of the major ions to one another) differs from that of seawater, and thus avoid the time-consuming step of characterizing the pH of the buffer for each new solution composition.
- A speciation model can address metrological concerns regarding traceability of the total pH scale to SI base units, and also quantify the present assumption that the activity coefficients of species involved in acid-base equilibria (Tris, TrisH^+ , H^+ , SO_4^{2-} , and HSO_4^-) are the same in the buffer solutions as in artificial seawater of the same nominal salinity ([Dickson et al., 2016](#)). Its practical effect is that, while total pH (operationally defined by [DelValls and Dickson \(1998\)](#)) is a measure of $([\text{H}^+] + [\text{HSO}_4^-])$, the relationship is not exact. There is a difference between the two which varies with both temperature and salinity, and very likely increases as salinity is reduced. This need not introduce any error into acid-base calculations as long as the stoichiometric dissociation constants in use – K_1 and K_2 of the carbonate system for example (e.g., [Dickson et al., 2007](#)) – are expressed on the same basis. However, it does mean that a total H^+ concentration determined from a measurement of seawater total pH, calibrated using the total pH values of [DelValls and Dickson \(1998\)](#), will not correspond to the conventional thermodynamic total $([\text{H}^+] + [\text{HSO}_4^-])$. (The latter quantity can be calculated directly by thermodynamic speciation models.) The magnitudes of the differences, and therefore the degree to which they are significant in any given application, are not yet known.
- The use of a speciation model to calculate the properties of buffer solutions, in particular electrolyte activities, would enable the

calibration of a H^+/Na^+ glass electrode pair, or a glass H^+ electrode paired with a Cl^- ion-specific electrode, for the measurement of hydrogen ion concentration in natural waters.

- A speciation model of artificial seawater that accurately calculates acid-base equilibria and pH can form the foundation of a model of seawater (that includes the carbonate system), with practical applications to problems of trace metal speciation and in ocean acidification (e.g., [Millero and Roy, 1997](#); [Pierrot and Millero, 2016](#)).

[Dickson et al. \(2016\)](#) suggested that such a model should be based on the Pitzer formalism ([Pitzer, 1991](#)) for the calculation of the activities of acid-base components in seawater media, together with a strategy for estimating their uncertainties.

Recently, [Humphreys et al. \(2022\)](#) have begun to address the requirements outlined above by implementing the [Waters and Millero \(2013\)](#) and [Clegg and Whitfield \(1995\)](#) Pitzer-based speciation models of artificial seawater within a generalised framework for solutions of arbitrary complexity, and including full propagation of uncertainties for the first time. A simplified approach to estimating the variances and covariances of the Pitzer activity coefficient interaction parameters was developed, thus allowing the calculation of both total uncertainties for all model outputs, and of all individual contributions to those uncertainties. The models were compared with the available electromotive force (EMF) data for acidified artificial seawater, with particular attention given to the determination of E^* , the standard EMF used in the definition of the total pH scale ([Dickson, 1990](#); [DelValls and Dickson, 1998](#)). The model of [Waters and Millero \(2013\)](#), with corrections, was adopted as the basis for further development. Recommendations were made for new thermodynamic measurements, and additions to the uncertainty treatment, to improve the model.

Here we extend the work of [Humphreys et al. \(2022\)](#), hereafter referred to as paper (I), to include the buffer species TrisH^+ and Tris for the temperature 25 °C. We compare the extended model to the EMF data for the Tris buffer solutions in artificial seawater that are used to define the total pH scale ([DelValls and Dickson, 1998](#)), and use the results of uncertainty calculations to identify the aqueous systems for which additional measurements are required to complete the model for the temperatures range 0 to 40 °C. We quantify, for the first time, the difference between total pH and $-\log_{10}([\text{H}^+] + [\text{HSO}_4^-])$ which is a key step in addressing the issues listed above. We show that the total pH scale is best extended to salinities below 20 by retaining the approach of [DelValls and Dickson \(1998\)](#) of substituting TrisH^+ for Na^+ in the artificial seawater medium. We also demonstrate the meaning of the empirical linear extrapolation of total pH to zero buffer molality in artificial seawater, which is of practical importance, and suggest a lower limit below which the relationship between pH and this molality becomes non-linear.

2. Extension of the speciation model to include Tris buffer

The artificial seawater proposed by [Dickson \(1990\)](#) contains the major ions Na^+ , Mg^{2+} , Ca^{2+} , K^+ , Cl^- and SO_4^{2-} . There are, in addition, the minor components H^+ , OH^- , MgOH^+ , and HSO_4^- that take part in acid-base equilibria. In section 2 of paper (I) we briefly summarised the available chemical speciation models, based upon the Pitzer equations for activity coefficients, for applications to natural waters. We also assessed the corrected model of [Waters and Millero \(2013\)](#), and that of [Clegg and Whitfield \(1995\)](#), for such an artificial seawater. Both models are fully described and documented in paper (I) and its associated Supporting Information. As noted in the previous section, the corrected model of [Waters and Millero \(2013\)](#) was adopted as the basis for future applications and development.

The Pitzer expressions for the activity coefficients (γ) of ions and uncharged species are described by [Pitzer \(1991, and references therein\)](#) and are not reproduced here. They include parameters, which vary with temperature and pressure, for the interactions of pairs and triplets of

Table 1
Sources of thermodynamic data for aqueous Tris, TrisHCl, and (TrisH)₂SO₄ solutions.

Data type ^a	Molality range (mol kg ⁻¹)	Temperatures (°C)	Source
Osmotic coefficients (Tris _(aq))	0.5035–5.889	25	Robinson and Bower (1965)
Osmotic coefficients (TrisHCl _(aq))	0.2781–7.805	25	Robinson and Bower (1965)
Osmotic coefficients ((TrisH) ₂ SO _{4(aq)})	0.1550–5.7742	25	Macaskill and Bates (1986)
EMF ($\gamma_{\text{TrisHCl}}/\gamma_{\text{Tris}}^{0.5}$)	0.0076–0.10	0–50	Bates and Hetzer (1961)
pH ₂ O (TrisHCl _(aq))	0.10–6.0	25–60	Lee and Lee (1998)
EDB (Tris _(aq))	2.819–20.25	20.4	Lodeiro et al. (2021)
aH ₂ O (Tris _(aq))	0.254–8.52	16–46	Unpublished ^b
C _p (TrisHCl _(aq))	0.00482–0.49621	5–120	Ford et al. (2000)
C _p (Tris _(aq))	0.00768–0.50768	5–120	Ford et al. (2000)

Notes

^a The osmotic coefficients were determined from isopiestic equilibrium with aqueous NaCl standards; the EMFs of these equimolar TrisHCl/Tris solutions yield the activity product of HCl, but can be analysed to yield the activity coefficient quotient indicated (see Eq. (6)); pH₂O are direct measurements of water vapour pressure above the indicated solutions; EDB are water activities determined from aqueous droplet evaporation rates in an electrodynamic balance; aH₂O are water activities measured with an AQUALAB water activity meter; C_p are apparent molar heat capacities (at 0.35 MPa).

^b Work by Tian Xiaomeng and Chak K. Chan of City University of Hong Kong.

solute species. The parameters for ion interactions are: $\beta_{ca}^{(0)}$, $\beta_{ca}^{(1)}$, $\beta_{ca}^{(2)}$, $C_{ca}^{(0)}$, and $C_{ca}^{(1)}$ for combinations of each cation *c* and each anion *a*; $\theta_{cc'}$ and $\psi_{cc'a}$ for each pair of dissimilar cations *c* and *c'*, and anion *a*; and $\theta_{aa'}$ and $\psi_{aa'c}$ for each pair of dissimilar anions *a* and *a'*, and cation *c*. The parameters for the self-interaction of Tris (the only neutral solute in the model of the buffer solution) are $\lambda_{\text{Tris,Tris}}$ and $\mu_{\text{Tris,Tris,Tris}}$, those for interactions between Tris and each ion *i* are $\lambda_{\text{Tris,i}}$, and interactions between Tris and each cation and anion are expressed by the parameter $\zeta_{\text{Tris,ca}}$. The interactions and parameters are summarised in the Glossary of Symbols.

The buffer solutions used to calibrate pH on the total scale (DelValls and Dickson, 1998) are prepared from artificial seawater, of various salinities, with added equimolar TrisH⁺ and Tris (such that TrisH⁺ replaces an identical molality of Na⁺). The inclusion of the buffer species in a speciation model of artificial seawater introduces the following additional elements: (i) the dissociation equilibrium between TrisH⁺

Table 2
Interaction parameters for modelling pK*(TrisH⁺) in salt solutions at 25 °C.

Ion M ^{z+}	$\theta_{H,M}$	$\psi_{H,M,Cl}$	$(\theta_{\text{TrisH,M}} - \lambda_{\text{Tris,M}})$
Na ⁺	0.0306	−0.004	−0.02632 ± 0.0015
Mg ²⁺	0.062	−0.011	0.1176 ± 0.019
Ca ²⁺	0.0612	−0.015	0.2686 ± 0.012
K ⁺	0.005	−0.011	−0.03394 ± 0.0046

Electrolyte	$\beta_{ca}^{(0)}$	$\beta_{ca}^{(1)}$	$C_{ca}^{(0)}$
HCl	0.17567	0.297786	0.0006874
TrisHCl ^a	0.0426783	0.196255	−0.00144509
(TrisH) ₂ SO ₄ ^b	0.095229 ±	0.58591 ±	−0.0015988 ±
	0.00050	0.020	0.000027

Solute	$\lambda_{\text{Tris,Tris}}$	$\mu_{\text{Tris,Tris,Tris}}$
Tris	−0.00516 ± 0.0010	0.000703 ± 0.00011

Notes: The listed $\theta_{H,M}$ and $\psi_{H,M,Cl}$ parameters, and those for HCl, are from the Waters and Millero (2013) model as amended in paper (I). The parameters for TrisHCl are from Lodeiro et al. (2021), and the combined $(\theta_{\text{TrisH,M}} - \lambda_{\text{Tris,M}})$ were fitted in this work. The value of the constant α is 2.0 for both TrisHCl and HCl. Values of the parameters $\lambda_{\text{Tris,TrisH}}$ (−0.01241) and $\lambda_{\text{Tris,SO}_4}$ (0.08245) were also adopted from Lodeiro et al. (2021).

^a The alternative parameters for TrisH⁺-Cl[−] interactions that were fitted, in Section 5.2 of this work, to data including osmotic coefficients determined from the EMFs of Bates and Hetzer (1961) are: $\beta^{(0)} = 0.03468 \pm 0.0047$, $\beta^{(1)} = 0.12802 \pm 0.0049$, $C^{(0)} = -0.0009366 \pm 0.00036$, $C^{(1)} = 0.09269 \pm 0.029$, $\alpha = 2.0$, $\omega = 2.5$.

^b The value of α is 2.0 for this pair of ions.

and Tris; (ii) cation-anion binary interactions between TrisH⁺ and Cl[−], SO₄^{2−}, and HSO₄[−]; (iii) neutral-neutral (self) interactions of Tris; (iv) neutral-ion interactions between Tris and the major cations and anions of artificial seawater; (v) cation-cation interactions between TrisH⁺ and the cations of artificial seawater; and (vi) several ternary interactions represented by parameters $\psi_{\text{TrisH,c,a}}$, $\psi_{a,a',\text{TrisH}}$ and $\zeta_{\text{Tris,c,a}}$ (where subscripts *c* and *a* represent the cations and anions present in artificial seawater). The data from which TrisH⁺-anion and Tris-Tris interaction parameters can be determined are summarised in Table 1, and are used in this work to extend the model of Waters and Millero (2013) at 25 °C.

The values of TrisH⁺-Cl[−] and Tris self-interaction parameters have been determined by Lodeiro et al. (2021) and are adopted here. We obtained values of the TrisH⁺-SO₄^{2−} parameters by fitting to osmotic coefficients measured by Macaskill and Bates (1986) (after recalculating values for the aqueous NaCl reference solutions using the work of Archer (1992)). These parameters are listed in Table 2. We set $\lambda_{\text{Tris,Cl}}$ to zero, as did Millero et al. (1987) and Lodeiro et al. (2021), because electro-neutrality constraints mean that Tris-ion parameters can only be determined as the combination $(\nu_+ \lambda_{\text{Tris,c}} + \nu_- \lambda_{\text{Tris,a}})$, where ν_+ and ν_- are stoichiometric numbers of the cation and anion in the salt. The interaction parameters $\lambda_{\text{Tris,TrisH}}$ and $\lambda_{\text{Tris,SO}_4}$, determined from solubility measurements, were taken from Lodeiro et al. (2021) and their values are given in the notes to our Table 2. Values for the other Tris-cation parameters were obtained by fitting the stoichiometric dissociation constants of TrisH⁺ ($K^*(\text{TrisH}^+)$) measured by Millero et al. (1987) in aqueous metal chloride solutions, using the following equation:

$$\ln(K^*(\text{TrisH}^+)) = \ln(K(\text{TrisH}^+)) + \{\text{TrisH}^+\text{-Cl}^- \text{ terms}\} - \{\text{H}^+\text{-Cl}^- \text{ terms}\} + 2mM^{z+} \cdot (\theta_{\text{TrisH,M}} - \theta_{\text{H,M}} - \lambda_{\text{Tris,M}}) + mM^{z+} \cdot m\text{Cl}^- \cdot (\psi_{\text{TrisH,M,Cl}} - \psi_{\text{H,M,Cl}} - \zeta_{\text{Tris,M,Cl}}) \quad (1)$$

where M^{z+} is one of the metal ions Na⁺, Mg²⁺, Ca²⁺, and K⁺, and prefix *m* denotes molality. The quantity $K(\text{TrisH}^+)$ (mol kg^{−1}) is the thermodynamic value of the dissociation constant. The relationship between thermodynamic and stoichiometric equilibrium constants is defined in the Glossary of Symbols. The terms for H⁺-Cl[−] and TrisH⁺-Cl[−] interactions in Eq. (1) are those that involve parameters $\beta_{ca}^{(0)}$, $\beta_{ca}^{(1)}$, and $C_{ca}^{(0)}$ for cations TrisH⁺ and H⁺, and anion Cl[−], and are listed in Table 2. The values of the mixture parameters $\theta_{H,M}$ and $\psi_{H,M,Cl}$ are also listed in the table. The terms in {} can be calculated using eqs. (63) and (64) of Pitzer (1991) or, alternatively, Eqs. (AI2) and (AI3) of Clegg et al. (1994).

It was found that the parameter pair ($\psi_{\text{TrisH,M,Cl}} - \zeta_{\text{Tris,M,Cl}}$) could be set to zero for all four salt solutions, leaving only the linear term $(\theta_{\text{TrisH,M}} - \lambda_{\text{Tris,M}})$ to be fitted. The fact that the two parameters cannot be distinguished does not influence calculations of buffer EMF (the

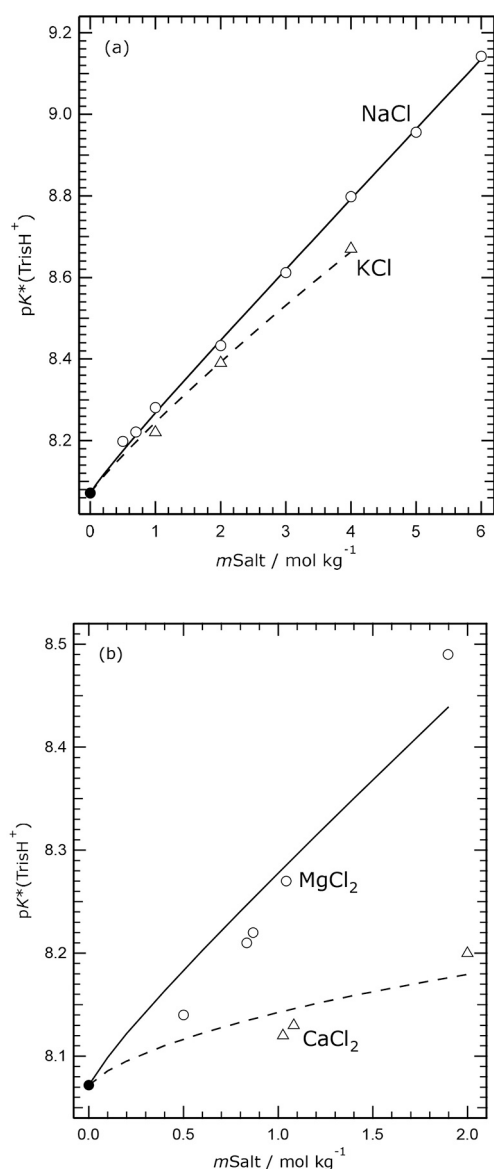


Fig. 1. Measured and fitted stoichiometric dissociation constants of TrisH⁺ ($pK^*(\text{TrisH}^+)$, equal to $-\log_{10}(K^*(\text{TrisH}^+))$), in various salt solutions at 25 °C, plotted against salt molality ($m\text{Salt}$). The symbols are the measurements of [Millero et al. \(1987\)](#), and the fitted values (lines) were obtained using Eq. (1). (a) NaCl – circle and solid line; KCl – triangle and dashed line. (b) MgCl₂ – circle and solid line; CaCl₂ – triangle and dashed line. The dot (both plots) is the thermodynamic value of $pK(\text{TrisH}^+)$. The stated uncertainty of the measurements is ± 0.005 in pK .

measurement used to calibrate the total pH scale) because they occur in those equations in the same combinations. In addition, for a buffer containing equimolar Tris and TrisH⁺, terms in $\lambda_{\text{Tris},\text{TrisH}}$ cancel, and the terms in $(\psi_{\text{TrisH},\text{M},\text{Cl}} - \zeta_{\text{Tris},\text{M},\text{Cl}})$ partially cancel and therefore have only a very small influence on calculated EMFs. The results of the fits are shown in [Fig. 1](#), and the fitted parameter combinations ($\theta_{\text{TrisH},\text{M}} - \lambda_{\text{Tris},\text{M}}$) are listed in [Table 2](#). Our analysis of the data is essentially the same as that of [Millero et al. \(1987\)](#), although we have fitted the measured $pK^*(\text{TrisH}^+)$ directly whereas Millero et al. first determined values of $\ln(\gamma_{\text{Tris}})$, see their [Fig. 3](#), and then obtained values of $\lambda_{\text{Tris},\text{M}}$ from linear fits ($\ln(\gamma_{\text{Tris}}) = 2mM^{2+} \cdot \lambda_{\text{Tris},\text{M}}$). We note that their value of $\lambda_{\text{Tris},\text{Mg}}$ (-0.0594) appears to be in error by a factor of 2 (its magnitude is too small).

There are no data from which to determine the parameters for TrisH⁺-HSO₄⁻ interactions at any temperature (and for most of the other

parameters mentioned above there are currently only data for 25 °C).

3. Treatment of uncertainties

Variances of model-predicted pH, activities, and other properties are calculated by standard methods of error propagation such as used by [Orr et al. \(2018\)](#). Their application to the speciation model used here is described in detail in paper (I). Values of the variances and covariances of the Pitzer interaction parameters are not available for the [Waters and Millero \(2013\)](#) model, and we adopted a simplified method of estimating them based upon the assumption that they were all determined from single datasets of osmotic coefficients (ϕ), which were assumed to be subject to the random and systematic errors that are typical of isopiestic measurements of water activity. This measurement is one of the main methods of activity determination for solutions of non-volatile electrolytes at room temperature and above ([Rard and Platford, 1991](#)). Parameter variances and covariances are determined from the statistics of multiple fits of artificial datasets of osmotic coefficients generated by the model and then perturbed by randomly generated errors both for individual points (random error) and affecting the entire artificial dataset (systematic error). Details are given in section 3 of paper (I), and in the Supporting Information to that work.

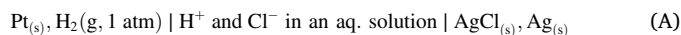
The above methods were applied to the additional cation-anion interactions (TrisH⁺-Cl⁻, TrisH⁺-SO₄²⁻, and TrisH⁺-HSO₄⁻) in the extension to the model, and the resulting variances and covariances can be found in the Supporting Information to this work with other details of the calculations. Pure aqueous Tris (interaction parameters $\lambda_{\text{Tris},\text{Tris}}$ and $\mu_{\text{Tris},\text{Tris},\text{Tris}}$) was treated in the same way, in the determination of parameter variances, as the single electrolytes.

The mixture parameter $\lambda_{\text{Tris},\text{Cl}}$ is set to zero by convention (and has a variance of zero) because these neutral-ion interaction parameters can only be determined in the combination $(\nu_+ \lambda_{\text{Tris},\text{M}} + \nu_- \lambda_{\text{Tris},\text{X}})$, where ν_+ and ν_- are the stoichiometric numbers of the two ions in the salt $M_{\nu_+}X_{\nu_-}$. Variances of $\lambda_{\text{Tris},\text{c}}$, where $c = \text{Na}^+, \text{Mg}^{2+}, \text{Ca}^{2+}, \text{K}^+$, and TrisH⁺ were determined from simulations of osmotic coefficients of solutions containing Tris and the chlorides of the above cations, and that of $\lambda_{\text{Tris},\text{SO}_4}$ from a simulation of Tris-(TrisH)₂SO₄ solutions. The approach was essentially the same as used to determine variances of ion-ion mixture parameters θ_{cc} , θ_{aa} , $\psi_{\text{cc}'\text{a}}$ and $\psi_{\text{aa}'\text{c}}$ in paper (I). Details are given in the Supporting Information. In the discussion in [Section 5.2](#), below, some comparisons are made between the variances of these neutral-ion and TrisH⁺-anion parameters determined by fitting and those estimated from simulations. We note that where parameter values have been determined from fits to single datasets – which is the case for all parameters involving Tris and TrisH⁺ in the model – the simulated parameter variances would generally be expected to be larger because they account for the possible influence of systematic error.

The variance of the equilibrium constant for TrisH⁺ dissociation in the model is set equal to the square of the uncertainty listed by [Bates and Hetzer \(1961\)](#) and given in our [Table 3](#) (see also the Supporting Information).

4. Data used to assess the model

Electromotive force measurements of Tris buffer solutions are used to evaluate the accuracy of the model. Comparisons with model predictions, including the use of the uncertainty propagation methods summarised above, enable us to determine the solute interactions and equilibrium constants that are most likely to cause the differences between measured and modelled EMFs. The sources of available data, summarised in [Table 4](#), are for the following electrochemical cell:



where the aqueous solution is an artificial seawater containing the buffer substance Tris and its protonated form TrisH⁺ (generally

Table 3

Values of the thermodynamic dissociation constant of TrisH^+ ($K(\text{TrisH}^+)$ / mol kg^{-1}) at 25 °C.

$10^9 K(\text{TrisH}^+)$	Uncertainty ^a	Type ^b	Reference
9.42	–	expt. ^c	Glasstone and Schram (1947)
8.395	–	expt. ^d	Bates and Pinching (1949)
8.4217	0.012	expt. ^e	Bates and Hetzer (1961)
8.4750	0.024	fitted ^f	Bates and Hetzer (1961)
8.4750	0.024	g	this work

Notes

^a The uncertainty in $10^9 K(\text{TrisH}^+)$, at 25 °C.

^b The 'Type' column indicates whether the listed value of $K(\text{TrisH}^+)$ is determined from experimental measurements ('expt. '), or from an equation fitted to experimental values ('fitted').

^c Obtained with a glass pH electrode, with results extrapolated to zero ionic strength. The value quoted was calculated using the value of pK_b (5.97) given by Glasstone and Schram (1947) and pK_w (where K_w is dissociation constant water) equal to 13.995, the same as used by Bates and Pinching (1949).

^d Electromotive force measurements using cell A. Values are also listed for 20 °C and 30 °C. Uncertainties are not quoted, but the value of pK_{bh} from which the listed $K(\text{TrisH}^+)$ is derived is given to four digits in the Table 4 of the cited reference.

^e Electromotive force measurements using cell A. Values were determined from 0 °C to 50 °C, at 5 °C intervals.

^f Calculated from eq. (3) of Bates and Hetzer (1961), which they fitted to their experimental data. The quoted uncertainty is calculated from the stated mean difference of ± 0.0012 in $-\log_{10}(K(\text{TrisH}^+))$ between the experimentally determined values and the fitted equation.

^g The value, and its associated uncertainty, determined by Bates and Hetzer (1961) are used (their Eq. (3)).

Table 4

Sources of electromotive force data for Tris buffers in artificial seawater (ASW).

Salinities	Ionic strengths ^a (mol kg^{-1})	t (°C)	Solution ^b	Ref.
30–40	0.616–0.831	5–40	Tris/TrisH ⁺ + ASW	Ramette et al. (1977)
35	0.723	5–45	Tris/TrisH ⁺ + ASW	Millero et al. (1993)
20–40	0.406–0.831	0–45	Tris/TrisH ⁺ + ASW	DelValls and Dickson (1998)
5–35	0.100–0.723	5–45	Tris/TrisH ⁺ + ASW ^c	Müller et al. (2018)
35	0.723	5–35	Tris/TrisH ⁺ + ASW	Pratt (2014)
35–100	0.723–2.214	–6–25	Tris/TrisH ⁺ + ASW	Papadimitriou et al. (2016)

Notes

^a These are formal ionic strengths that do not take into account any ion-pairing (see Khoo et al., 1977) or the formation of HSO_4^- in the solutions of artificial seawater with added HCl.

^b Artificial seawater is denoted by ASW. The Tris and TrisH^+ are generally equimolar, except for some measurements by Bates and Pinching (1949) for Tris/TrisHCl solutions, and in the work of Pratt (2014) cited above. The ions H^+ and TrisH^+ are substituted for Na^+ in all the studies in artificial seawater, but see note (c) below.

^c In this study the artificial seawater recipe was modified so that, on the addition of TrisH^+ , a constant ionic strength was maintained. However, the ratios of the molalities of seawater ions to each other differ from those in artificial seawater (eq. (1) of Müller et al., 2018), and also do not extrapolate to the composition of artificial seawater in the limit of zero added buffer.

substituted for Na^+). The EMF, E (V), of cell A is given by:

$$E = E^0 - (RT/F) \cdot \ln(a\text{H}^+ \cdot a\text{Cl}^-) \quad (2)$$

where E^0 (V) is the standard EMF of the cell at the temperature T (K) of interest, R (8.31446 J mol⁻¹ K⁻¹) is the gas constant, F (96,485.332 C mol⁻¹) is the Faraday constant, and prefix a denotes activity. The

activity product of the H^+ and Cl^- ions can also be written $m\text{H}^+ \cdot m\text{Cl}^- \cdot \gamma_{\text{H}^+} \cdot \gamma_{\text{Cl}^-}$ or $m\text{H}^+ \cdot m\text{Cl}^- \cdot \gamma_{\text{HCl}}^2$, where γ_i is the activity coefficient of solute species i , and γ_{HCl} is the mean activity coefficient of H^+ and Cl^- in the aqueous solution (γ_{HCl} is equal to $(\gamma_{\text{H}^+} \cdot \gamma_{\text{Cl}^-})^{0.5}$).

Measurements of these buffer solutions, in combination with those of artificial seawater acidified with varying molalities of HCl, are the basis of the total pH scale (Dickson, 1990; DelValls and Dickson, 1998).

For solutions of Tris buffer in artificial seawater the activity of H^+ in Eq. (2) for the EMF of the solution can be replaced, yielding:

$$E = E^0 - (RT/F) \cdot \ln(K(\text{TrisH}^+) \cdot a\text{TrisH}^+ \cdot a\text{Cl}^- / a\text{Tris}) \quad (3)$$

where $K(\text{TrisH}^+)$ is the thermodynamic equilibrium constant for the acid dissociation of TrisH^+ , which can be calculated as a function of temperature using eq. (3) of Bates and Hetzer (1961). There are three important characteristics of these solutions in relation to the cell EMFs: (i) the molalities of TrisH^+ and Tris, in solutions prepared with similar molalities of each species, remain almost unaltered by the equilibrium; (ii) $m\text{H}^+$ is negligible compared to $m\text{TrisH}^+$ and $m\text{Tris}$ (both are typically 0.04 mol kg^{-1}), and (iii) $m\text{HSO}_4^-$ is negligible compared to $m\text{SO}_4^{2-}$. Together, these mean that the EMFs of typical Tris buffer solutions in artificial seawater, including those from sources listed in Table 4, are not affected by the $\text{SO}_4^{2-}/\text{HSO}_4^-$ equilibrium. Comparisons of modelled and measured EMFs are therefore entirely a test of the model's ability to represent the activity product $a\text{TrisH}^+ \cdot a\text{Cl}^- / a\text{Tris}$, and the accuracy with which the equilibrium constant is known.

The uncertainties of EMF measurements, in particular those of acidified artificial seawater made by Khoo et al. (1977), Dickson (1990), and Campbell et al. (1993) are considered in detail in section 4.1 of paper (I). Estimated standard uncertainties were approximately 0.04 mV in all cases, consistent with the finding of Dickson (1990) that measurements generally agreed to within 0.05 mV. A similar analysis of the experiments of DelValls and Dickson (1998), given in detail in the Supporting Information to this work, also yields 0.04 mV.

5. Assessment of the model

In this section we compare the model with available EMFs of the Tris buffer solutions, and identify the causes of the differences found. The parameters for the $\text{TrisH}^+ \text{-Cl}^-$ interaction are revised, to improve agreement. We identify the different components of the variation of EMF with buffer molality at constant salinity measured by DelValls and Dickson (1998), and determine the reason for its linearity at all but the lowest molalities of buffer. We explain the meaning of a linear extrapolation of measured EMF to zero buffer molality (equivalent to what is shown in fig. 1 of DelValls and Dickson (1998)). The effect of varying the ratio $\text{TrisH}^+:\text{Tris}$ in the buffer solutions is examined and it is shown that the effect on EMF can be calculated to within experimental uncertainty by a simple expression involving only the molalities of the two species. All comparisons are made at 25 °C, because the Pitzer interaction parameters involving TrisH^+ and Tris are known only at this temperature.

5.1. Calculations of uncertainty contributions to modelled quantities

We first carried out a model simulation to determine the relative contributions of the uncertainties in the equilibrium constants and interaction parameters to those of calculated EMFs. This simulation was for equimolar Tris/TrisH⁺ buffer in artificial seawater of salinity 35. The composition of the solution is listed in Table 5.

As noted earlier, the variances and covariances of $\text{TrisH}^+ \text{-Cl}^-$ and $\text{TrisH}^+ \text{-SO}_4^{2-}$ parameters were simulated in the same way as for the other pure electrolytes, to ensure consistency, even though uncertainties of the parameters are available from the original fits used to determine their values. For both electrolytes there is only a single data set of osmotic coefficients, thus they correspond quite closely to the idealised case being examined here. The simulated variances of the interaction

Table 5

Solution compositions for artificial seawaters (ASW) of salinity 35, and Tris/TrisH⁺ buffer in artificial seawater.

Solute species	ASW (mol kg ⁻¹)	ASW (mol kg ⁻¹)	Tris/TrisH ⁺ buffer in ASW (mol kg ⁻¹)
H ⁺	– ^a	– ^a	–
Na ⁺	0.48516	0.48618	0.44618
Mg ²⁺	0.05518	0.05474	0.05474
Ca ²⁺	0.01077	0.01075	0.01075
K ⁺	0.01058	0.01058	0.01058
TrisH ⁺	–	–	0.040 ^a
Cl ⁻	0.56912	0.56920	0.56920
SO ₄ ²⁻	0.02926	0.02927	0.02927
Tris	–	–	0.040

Notes: The composition in the first column of molalities is from Khoo et al. (1977), and the second is from Dickson (1990). The composition of the buffer (last column) is the same as for the artificial seawater of Dickson, but with TrisH⁺ substituted for Na⁺, and Tris added. Ramette et al. (1977) used the recipe of Khoo et al. (1977) in their experiments.

^a For EMF measurements of acidified artificial seawater, H⁺ (of various molalities) is substituted for Na⁺, and for measurements of buffer solutions TrisH⁺ is substituted for Na⁺.

parameters $\lambda_{\text{Tris},i}$, where i is Na⁺, Mg²⁺, Ca²⁺, K⁺, TrisH⁺ or SO₄²⁻ were either similar in magnitude to those determined from the fits to the data (in the cases of $\lambda_{\text{Tris},\text{Na}}$ and $\lambda_{\text{Tris},\text{TrisH}}$) or up to two orders of magnitude smaller (in particular $\lambda_{\text{Tris},\text{Mg}}$ and $\lambda_{\text{Tris},\text{Ca}}$). Covariances of the Tris self-interaction parameters were also simulated for these calculations and found to be about 0.25 times the values obtained by Lodeiro et al. (2021) from a fit to the single available osmotic coefficient dataset of Robinson and Bower (1965).

There are some other special features of the parameters $\lambda_{\text{Tris},c}$, $\theta_{\text{TrisH},c}$, and $\psi_{\text{TrisH},c,\text{Cl}}$ for the seawater cations c . The measurements of $\text{p}K^*(\text{TrisH}^+)$ in chloride media at 25 °C yield values of parameter combinations ($\theta_{\text{TrisH},c} - \theta_{\text{H},c} - \lambda_{\text{Tris},c}$) and ($\psi_{\text{TrisH},c,\text{Cl}} - \psi_{\text{H},c,\text{Cl}} - \zeta_{\text{Tris},c,\text{Cl}}$), see Eq. (1) above. The parameter contributions to the calculated EMF of a Harned cell containing equimolar Tris/TrisH⁺ buffer occur in essentially the same combinations, although with the addition of a few smaller terms. Our fits above, and those of Millero et al. (1987), yielded ($\psi_{\text{TrisH},c,\text{Cl}} - \zeta_{\text{Tris},c,\text{Cl}}$) equal to zero. We also set all other ternary interaction parameters $\zeta_{\text{Tris},c,a}$ to zero, for simplicity. This implies that $\ln(\gamma_{\text{Tris}})$ is a linear function of the molality of dissolved salts, which is reasonable for solutions of seawater concentrations. In our calculations we assigned the fitted values of ($\theta_{\text{TrisH},c} - \lambda_{\text{Tris},c}$) to $\lambda_{\text{Tris},c}$, as did Millero et al. (1987), and therefore set the values and variances of $\theta_{\text{TrisH},c}$ to zero. In the calculations of uncertainties using these variances (and shown in figures) we ascribe the variance contribution of each $\lambda_{\text{Tris},c}$ to ($\lambda_{\text{Tris},c} - \theta_{\text{TrisH},c}$) in order to make this assignment clear.

Two sets of calculations were carried out to estimate uncertainty contributions to modelled EMFs and, in later sections, to other quantities such as total pH. In the first set the variances and covariances of parameters whose values are set to zero in the model are also set to zero in most instances. These parameters are listed in Tables S2–S5 in the Supporting Information to both this work and to paper (I) and include, for example, $\theta_{\text{HSO}_4,\text{SO}_4}$ and those for interactions between pairs of reacting species such as TrisH⁺ and OH⁻, and H⁺ and MgOH⁺. There are also parameters for interactions that are unknown because of a lack of data from which to determine them. These are assigned values of zero by default, but may in reality be non-zero. Their variances can be simulated in the same way as for other parameters, based on an assumption that their true values are zero, and this has been done in some cases. We carried out the second set of uncertainty simulations in order to explore the influence of these model parameters, identified by ‘U’ in Tables S2–S5 in the Supporting Information to both this work and paper (I), in a more realistic way. In this case we substituted mean parameter values for charge types corresponding to those of the interacting ions from Tables A1 and A2 in Appendix A of paper (I), and set their variances

equal to the squares of the listed standard deviations. We have not attempted to estimate covariances of, for example, unknown θ_{ij} and ψ_{ij} parameters whose values are generally determined simultaneously. This will tend to increase their contributions to the total uncertainty. This substitution of non-zero parameter values into the model means that the calculated quantities – both speciation and activity coefficients – will be different from the base model. However, the differences are found to be very small.

5.2. Equimolar TrisH⁺/Tris buffer in artificial seawater

An uncertainty profile for the calculated EMF difference ($E - E^0$) of a 0.04 mol kg⁻¹ equimolar TrisH⁺/Tris buffer in artificial seawater at salinity 35 is plotted in Fig. 2. This diagram shows the percentage contributions to the total modelled variance of the EMF of individual Pitzer interaction parameters, groups of related parameters, and individual equilibrium constants. The principal contribution is the TrisH⁺-Cl⁻ interaction, followed by Na⁺-Cl⁻ (less than 20% of the total estimated variance), and then by $\ln(K(\text{TrisH}^+))$ (about 5%). The HSO₄⁻/SO₄²⁻ equilibrium does not affect the EMF to any measurable extent in these buffer solutions, and does not contribute to the estimated uncertainty, for reasons given in the previous section.

A notable feature of Fig. S1 in the Supporting Information, which shows the partial derivatives of the calculated EMF, is the large value for $\lambda_{\text{Tris},\text{Na}}$ even though this parameter only contributes 1% to the total variance (as $(\lambda_{\text{Tris},\text{Na}} - \theta_{\text{TrisH},\text{Na}})$). The value of the variance of this combined parameter used in the calculations is equivalent to a standard deviation of 0.0014. We obtained a standard deviation of 0.0015 in our fit of the $\text{p}K^*(\text{TrisH}^+)$ measurements of Millero et al. (1987), essentially the same as used in the model. Thus it is likely that the modelled uncertainty contribution of this pair of parameters is reasonable.

A further set of calculations were carried out in which two changes were made: first, parameters whose values are unknown were assigned average values and associated uncertainties from Tables A1 and A2 from the Appendix to paper (I). In addition to the many $\psi_{cc'a}$ and $\psi_{aa'c}$

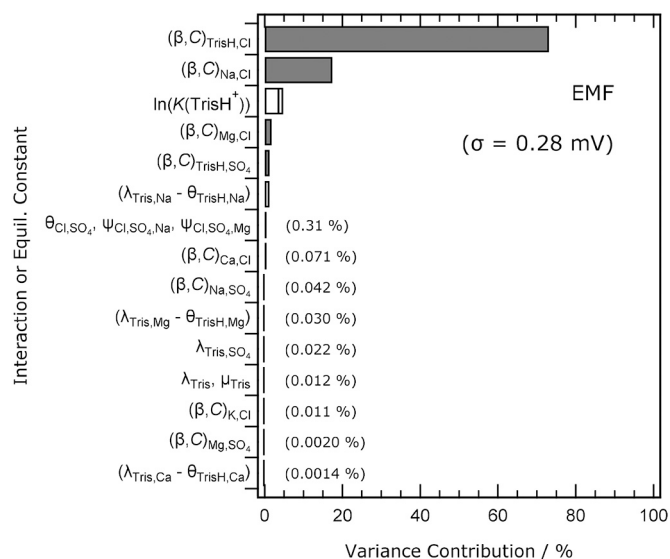


Fig. 2. Percentage contributions of individual Pitzer model interactions, and equilibrium constants, to the variance of the calculated EMF (Eq. (2)) at 25 °C of a Harned cell containing 0.04 mol kg⁻¹ equimolar TrisH⁺/Tris buffer in artificial seawater of salinity 35. The parameters associated with each of the interactions are listed down the lefthand side, and contributions of <1% and below are noted on the plot. Symbol $K(\text{TrisH}^+)$ denotes the thermodynamic dissociation constant of TrisH⁺. Only the fifteen largest contributions are shown, and interactions with very small variance contributions are omitted. The standard uncertainty of the calculated EMF is noted on the plot.

parameters for which this was done, there are also the unknown cation-anion interactions $\text{MgOH}^+\text{-SO}_4^{2-}$ and $\text{TrisH}^+\text{-HSO}_4^-$. Second, the variances of $(\lambda_{\text{Tris},c} - \theta_{\text{TrisH},c})$ for all cations c , and $\lambda_{\text{Tris},\text{SO}_4}$, were set to the uncertainties obtained from the fits to data (Table 2). As noted above, the variance for $(\lambda_{\text{Tris},\text{Na}} - \theta_{\text{TrisH},\text{Na}})$ is virtually unchanged, but for $(\lambda_{\text{Tris},\text{Mg}} - \theta_{\text{TrisH},\text{Mg}})$ it is a factor of 100 higher, and for $(\lambda_{\text{Tris},\text{Ca}} - \theta_{\text{TrisH},\text{Ca}})$ and $(\lambda_{\text{Tris},\text{K}} - \theta_{\text{TrisH},\text{K}})$ it is higher by factors of 40 and 10 respectively. The variance of $\lambda_{\text{Tris},\text{SO}_4}$ is increased by just over a factor of 2 relative to the base case. The calculated EMF of the buffer, at salinity 35, differed by only 0.007 mV from the base case calculation, and the total calculated variance was 4.1% greater than for the base case, almost all of which is accounted for by the increased variance contributions of the Tris-ion interaction parameters noted above. They contributed about 1.27% of the total variance in the base case calculations and 5.1% in the second case. The parameter pair $(\lambda_{\text{Tris},\text{Mg}} - \theta_{\text{TrisH},\text{Mg}})$ accounts for only 0.03% of the estimated total variance in the base case calculation, but about 3.6% in the second case (just less than the 4.6% attributed to $\ln(K(\text{TrisH}^+))$). The parameter pair $(\lambda_{\text{Tris},\text{Na}} - \theta_{\text{TrisH},\text{Na}})$ is the next most important Tris interaction parameter, accounting for 1.5% of the total variance in the second case. The reasons that $(\lambda_{\text{Tris},\text{Mg}} - \theta_{\text{TrisH},\text{Mg}})$ dominate are, first, the interaction of Mg^{2+} with Tris is very strong and, second, there are fewer (and more scattered) data points from which to determine its value than is the case for Na^+ (see Fig. 1). The only other changes in variance contributions from the second calculation, relative to that shown in Fig. 2, are below 0.1% of the total.

Overall, these comparisons show, first, that the estimated variance of the calculated EMF is dominated by only a very few terms, and that interactions involving the SO_4^{2-} ion have very little influence. Second, the unknown interaction parameters for this chemical system are also expected to have relatively little effect, but some changes to the magnitudes and ordering of variance contributions can be expected when actual rather than simulated parameter variances are used.

Electromotive forces measured by DelValls and Dickson (1998) and Ramette et al. (1977) are compared, as $(E - E^0)$, with calculated values in Fig. 3. There is a difference of about 0.6 to 0.8 mV from the measured values of DelValls and Dickson at all salinities and all added molalities of Tris and TrisH^+ . This exceeds the estimated uncertainties of the calculated EMFs (the shaded areas in the figures). The difference between the two data sets, about 0.3 mV, has been discussed by DelValls and Dickson, who suggest that the Tris stock solution of Ramette et al. (which was common to all of their experiments) may have been incorrectly characterized. Using the relationship between buffer composition and EMF discussed in Section 5.4 it is possible to show that the 0.3 mV difference at 25 °C corresponds to a Tris molality in the buffer that is too low by just over 1% relative to TrisH^+ . However, it is probable that the reasons for the differences will never be known.

What is the likely cause of the large deviations of calculated from measured values in Fig. 3? The uncertainty profile in Fig. 2 shows that the $\text{TrisH}^+\text{-Cl}^-$ parameters have the largest contribution to the total variance. The data from which these were obtained are eleven osmotic coefficients from isopiestic measurements by Robinson and Bower (1965). There are only two data points below 1 mol kg⁻¹ molality, and the fitted model closely represents the data. The only other measurements with which comparisons are possible are the EMFs of equimolar TrisHCl/Tris solutions up to 0.1 mol kg⁻¹ molality determined by Bates and Hetzer (1961) and used to derive the thermodynamic equilibrium constant $K(\text{TrisH}^+)$. In these solutions the measured EMFs are related to the mean activity coefficient of TrisHCl (γ_{TrisHCl}) by:

$$2\ln(\gamma_{\text{TrisHCl}}) - \ln(\gamma_{\text{Tris}}) = - (E - E^0)F/(RT) - \ln(K(\text{TrisH}^+) \cdot m\text{TrisH}^+ \cdot m\text{Cl}^- / m\text{Tris}) \quad (4)$$

In the dilute solutions measured by Bates and Hetzer (1961) the values of γ_{Tris} will be close to unity and have only a small contribution to the EMF, which can be accounted for using Pitzer parameters for 25 °C presented by Lodeiro et al. (2021) in their Table 8. (The mutual

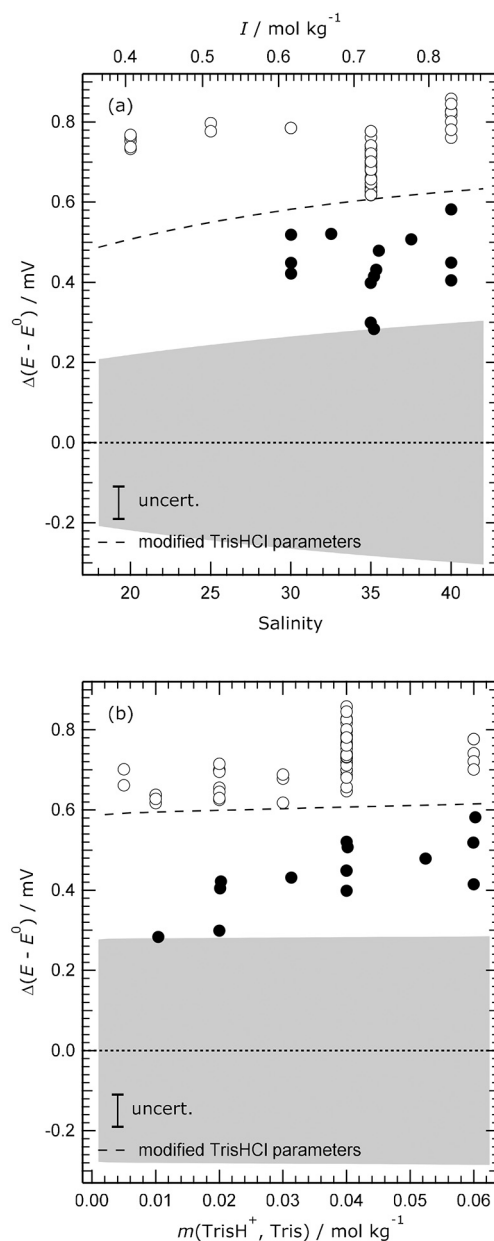


Fig. 3. Measured and modelled properties of artificial seawater containing equimolar TrisH^+ /Tris (various molalities), at 25 °C. (a) Differences between measured and calculated EMFs ($\Delta(E - E^0)$), plotted against salinity (bottom axis) and ionic strength (I) (top axis). Symbols: dot – measurements of Ramette et al. (1977); circle – measurements of DelValls and Dickson (1998). The shaded area shows the total uncertainty in the calculated value of $(E - E^0)$, and is centered on the zero line. The dashed line represents the position of $\Delta(E - E^0)$ equal to zero for the case where modified $\text{TrisH}^+\text{-Cl}^-$ parameters are used (described later in the ms), i.e. deviations are reduced by about 0.5 to 0.6 mV for this case. (b) The same data as in (a), but plotted against the molalities of TrisH^+ and Tris in the solutions ($m\text{TrisH}^+$, $m\text{Tris}$) for all salinities. The dashed line has the same meaning as in (a). The corrected model of Waters and Millero (2013), described in paper (I) and with additions presented in this work, was used in these calculations. The estimated uncertainties in the measured $(E - E^0)$ (i.e., \pm one standard deviation) are indicated on the plots.

interaction of TrisH^+ and Tris, expressed by the parameter $\lambda_{\text{Tris},\text{TrisH}}$, cancels in these equimolar solutions.) In order to compare the EMF data to the available coefficients of aqueous TrisHCl we first fitted values of $\ln(\gamma_{\text{TrisHCl}})$ calculated from Eq. (4) above using the Pitzer Debye-Hückel expression and the model term containing the single

interaction parameter $\beta^{(0)}_{\text{TrisHCl}}$ (Pitzer, 1991). We then derived a set of pseudo-experimental osmotic coefficients (ϕ_E) of pure aqueous TrisHCl using the following relationship (e.g., Pitzer, 1995):

$$\phi_E = \ln(\gamma_{\text{TrisHCl}}) + 1 - \int_0^m (\phi - 1)/m \, dm \quad (5)$$

The value of the osmotic coefficient of pure aqueous TrisHCl, at its molalities in the mixtures measured by Bates and Hetzer, was calculated using the Pitzer equation with the fitted parameter $\beta^{(0)}_{\text{TrisHCl}}$. This is

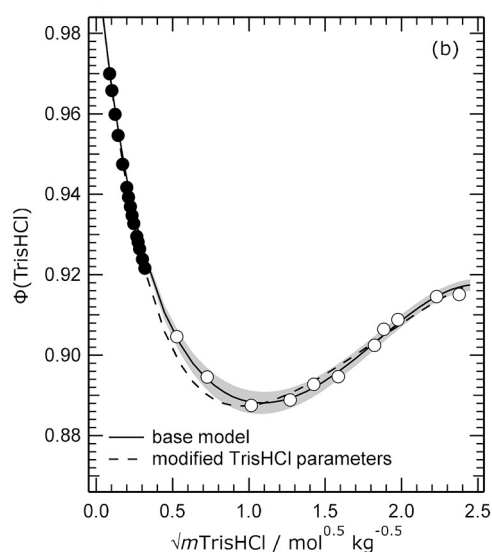
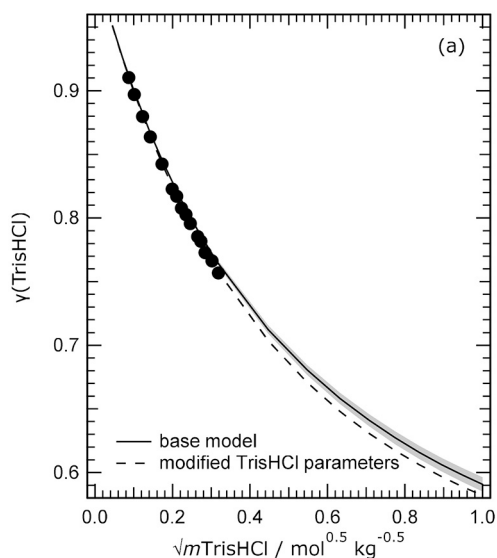


Fig. 4. Activity and osmotic coefficients of pure aqueous TrisHCl at 25 °C. (a) Mean activity coefficients ($\gamma(\text{TrisHCl})$) plotted against the square root of TrisHCl molality ($\sqrt{m\text{TrisHCl}}$). Symbols – determined from the EMF measurements of equimolar TrisHCl/Tris solutions of Bates and Hetzer (1961) (see text). Lines: solid – calculated using the present model (shaded area indicates uncertainty), which is based upon the osmotic coefficients determined by Robinson and Bower (1965); dashed – calculated using alternative model parameters that were constrained using the measurements of Bates and Hetzer (1961) in addition to the osmotic coefficients of Robinson and Bower (1965). (b) Osmotic coefficients ($\phi(\text{TrisHCl})$) plotted against the square root of TrisHCl molality. Symbols: dot – determined from the EMF measurements of Bates and Hetzer (1961); circle – isopiestic measurements of Robinson and Bower (1965). Lines: solid – the present model (shaded area indicates uncertainty); dashed – alternative model that is constrained to fit the values determined from the EMF data.

equivalent to the right-hand side of Eq. (5). The fitted values of $\ln(\gamma_{\text{TrisHCl}})$ at each experimental molality were then subtracted, and the values of $\ln(\gamma_{\text{TrisHCl}})$ obtained from the measurements of Bates and Hetzer added, to yield ϕ_E .

Both $\ln(\gamma_{\text{TrisHCl}})$ and ϕ_E determined from the study of Bates and Hetzer (1961) are shown in Fig. 4, and compared with values calculated using the present model (solid line) and also the osmotic coefficients measured by Robinson and Bower (1965). The activity and osmotic coefficients derived from the results of Bates and Hetzer are not consistent with work of Robinson and Bower, and lie outside of the estimated envelope of uncertainty (the shaded areas in the figure).

In order to determine whether this discrepancy would explain the 0.6 to 0.8 mV difference between measured and calculated EMFs of Tris buffers, we first refitted a combined dataset of ϕ_E and experimental osmotic coefficients of Robinson and Bower, with weights assigned so that ϕ_E was represented very closely. The modified interaction parameters are listed in the notes to Table 2. The resulting osmotic and mean activity coefficients are shown as dashed lines in Fig. 4. The new values of γ_{TrisHCl} are lower, by up to about 0.01, over much of the molality range. Next, EMFs of the Tris buffer solutions were recalculated using the revised set of parameters for $\text{TrisH}^+\text{-Cl}^-$ interactions. The change is shown in Fig. 5 as values of $\gamma_{\text{TrisHCl}} / (\gamma_{\text{Tris}})^{0.5}$, calculated from the measured EMFs, for solutions containing 0.04 mol kg^{-1} buffer. There is improved agreement of the model with the data across the salinity range. The deviations of the measured from calculated ($E - E^0$) shown in Fig. 3 are reduced from an average of 0.726 mV to only 0.13 ± 0.07 mV, which is a large improvement. The fine dashed lines in Fig. 3 show where $\Delta(E - E^0)$ equals zero when the calculation is carried out with the revised $\text{TrisH}^+\text{-Cl}^-$ parameters. For example, at salinity 35 (in Fig. 3a)

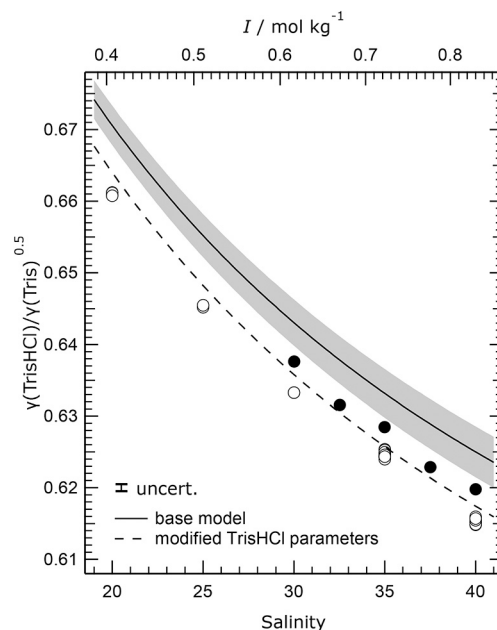


Fig. 5. Mean activity coefficients of TrisHCl divided by the square root of the Tris activity coefficient ($\gamma_{\text{TrisHCl}}/\gamma_{\text{Tris}}^{0.5}$), determined from measured EMFs of artificial seawater containing 0.04 mol kg^{-1} equimolar TrisH^+ /Tris buffer. See Eq. (4). The values are plotted against salinity (bottom axis) and the corresponding ionic strengths (I) (top axis). Symbols: dot – measurements of Ramette et al. (1977); circle – measurements of DelValls and Dickson (1998). Lines: solid – calculated using the Waters and Millero (2013) model (and $\text{TrisH}^+\text{-Cl}^-$ interaction parameters listed in Table 2); dashed – calculated using the same model but with $\text{TrisH}^+\text{-Cl}^-$ parameters refitted to agree closely with the EMFs of Bates and Hetzer (1961) (and given in the notes to Table 2). Shaded area – range of uncertainty in the activity coefficient quotient calculated using the model. The estimated uncertainty in the measured y variable (i.e., \pm one standard deviation) is indicated on the plot.

the deviations of the measurements of DelValls and Dickson (1998) from calculated values are reduced to about 0 to 0.16 mV (from the previous 0.62 to 0.78 mV) by using the revised parameters.

A further possible cause of the difference between measured and modelled EMFs is the value of $K(\text{TrisH}^+)$. The values of $\ln(K(\text{TrisH}^+))$ used in our model are calculated using eq. (3) of Bates and Hetzer (1961), and their uncertainty is ± 0.0028 (see Table 3). A refit of the experimental EMFs of Bates and Hetzer (1961) at 25 °C, using their method but with the Pitzer model Debye-Hückel expression and modern values of the constants R and F , yields $\ln(K(\text{TrisH}^+))$ that is lower than the value in Table II of Bates and Hetzer by 0.0028, and lower than the value obtained from their Eq. (3) by 0.0092. These differences are equivalent to an increase in the calculated EMFs of the buffer solutions studied by DelValls and Dickson (1998) of 0.073 mV to about 0.25 mV (which reduces the differences in $(E - E^0)$ and $\gamma_{\text{TrisHCl}}/(\gamma_{\text{Tris}})^{0.5}$ shown in Figs. 3 and 5, respectively).

It is concluded from these comparisons that a revision of the $\text{TrisH}^+ - \text{Cl}^-$ interaction parameters is needed, preferably based upon further measurements. These might include measurements of EMFs of Tris buffers in NaCl media, although from such mixtures some interaction parameters can only be determined in combination, and not individually. Revisions to the thermodynamic values of the TrisH^+ dissociation constant should also be considered.

5.3. Variation of buffer molality in equimolar $\text{TrisH}^+/\text{Tris}$ buffers in artificial seawater

The differences between modelled and calculated EMFs and $\gamma_{\text{TrisHCl}}/(\gamma_{\text{Tris}})^{0.5}$ for solutions containing the buffer have been shown in Figs. 3 and 5 to vary little with salinity, and to be greatly improved by revisions of the $\text{TrisH}^+ - \text{Cl}^-$ parameters. It is also important to be able to model accurately the variation of the EMF with the molality of the added buffer (at fixed salinities), because this is central to the extrapolation of the EMF and pH of buffer solutions to trace values appropriate to pure artificial seawater media, and to quantifying the influence of the buffer substances on the activity coefficients that control the measured EMF. For example, see fig. 1 of DelValls and Dickson (1998) which shows a decrease of about 0.0025 units in total pH from 0.04 mol kg⁻¹ buffer to the hypothetical case of zero added buffer (for salinity 35 and 25 °C). This change is equivalent to a decrease of about 0.16 mV in EMF (table 2 of DelValls and Dickson).

How well can the model represent this change with buffer molality, what does it mean, and should the relationship be linear? To answer these questions we first rearrange Eq. (3) to express the EMFs of the solutions as the sum of four terms:

$$E - E^0 = - (RT/F) \{ \ln(K(\text{TrisH}^+)) + \ln(\gamma_{\text{TrisH}^+} \gamma_{\text{Cl}^-} / \gamma_{\text{Tris}}) + \ln(m\text{TrisH}^+ / m\text{Tris}) + \ln(m\text{Cl}^-) \} \quad (6)$$

In this equation $K(\text{TrisH}^+)$ is a constant for any given temperature, and $m\text{Cl}^-$ is constant at any particular salinity. In typical buffer solutions prepared with equimolar TrisH^+ and Tris, the molalities of the two species can be shown to be very close to their nominal values. However, this approximation becomes less exact at very low molalities of buffer, which has implications for the extrapolation of EMFs and pH as will be demonstrated.

Fig. 6 shows EMFs of a salinity 35 buffer at 25 °C measured by DelValls and Dickson (1998). The data correspond to the total pH values shown in their fig. 1. The dotted line is a simple linear fit to the data. The solid line represents EMFs calculated using the model and Eq. (6) above. Note that it has been shifted vertically on the plot by +0.095 mV, in order to aid comparison of the slopes. (In the model we used the revised $\text{TrisH}^+ - \text{Cl}^-$ parameters derived in Section 5.2.) The calculated relationship between EMF and buffer molality below about 0.02 mol kg⁻¹ is highly non-linear, because as buffer molality tends to zero the H^+ molality tends to a value of about 1.97×10^{-7} mol kg⁻¹ in the pure

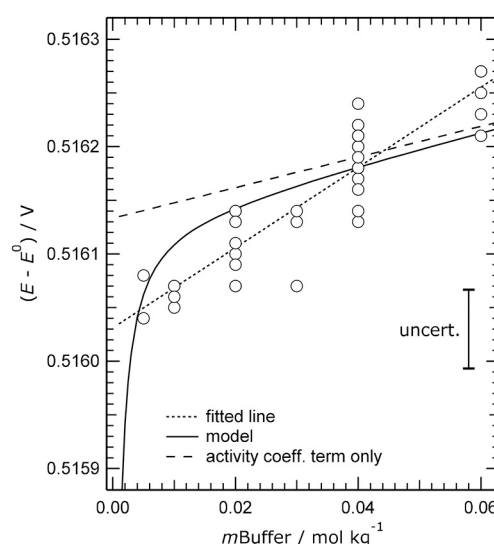


Fig. 6. Measured and calculated EMFs ($E - E^0$) of equimolar $\text{TrisH}^+/\text{Tris}$ buffer in artificial seawater of salinity 35 at 25 °C, plotted against the molality of the buffer (m_{Buffer}). Symbols: data of DelValls and Dickson (1998). Lines: dotted – linear fit of the measured ($E - E^0$); solid – calculated using the model of Waters and Millero (2013), with additional the TrisH^+ and Tris interaction parameters derived in section 2.1 (and with $\text{TrisH}^+ - \text{Cl}^-$ parameters refitted to agree closely with the EMFs of Bates and Hetzer (1961)); dashed – the activity coefficient term only (see Eq. (6)), calculated using the same parameters as for the solid line. Note that both solid and dashed lines have been shifted vertically by +0.095 mV so that the solid line agrees with the fitted line (dotted line) at 0.04 mol kg⁻¹ of buffer. The estimated uncertainty in the measured ($E - E^0$) (i.e., \pm one standard deviation) is indicated on the plot.

artificial seawater (as determined by the model). This corresponds to an ($E - E^0$) of about 0.4286 V. Above 0.02 mol kg⁻¹ of buffer the slope of the calculated EMFs with respect to buffer molality is less than what is observed, which we attribute to deficiencies in the model. It is important to understand that the EMF at trace buffer molality, obtained by the linear extrapolation of the measured EMFs in Fig. 6 (about 0.51603 V, dotted line) does not have the same meaning or value as the EMF of a pure artificial seawater solution containing no (i.e., zero) buffer (about 0.4286 V, stated above). The same is true of the corresponding total pH (fig. 1 of DelValls and Dickson, 1998).

Eq. (6) shows that there are two contributions to the change of EMF with buffer molality, and the model can be used to quantify and compare them. First, the dashed line in Fig. 6 shows the EMF calculated using Eq. (6), but neglecting the term in $\ln(m\text{TrisH}^+ / m\text{Tris})$. It represents the effect of the changing activity coefficient contribution ($-(RT/F) \cdot \ln(\gamma_{\text{TrisH}^+} \gamma_{\text{Cl}^-} / \gamma_{\text{Tris}})$) on EMF, and how it varies with buffer molality. The second contribution to the change in EMF is represented by the small difference between the dashed and solid lines in Fig. 6 and is the effect of the change in the equilibrium ratio $m\text{TrisH}^+ / m\text{Tris}$ with buffer molality. For 0.02 mol kg⁻¹ of buffer and above, the magnitude of this contribution in Eq. (6) is no more than about 0.02 mV, which is less than the uncertainty in the measurements. Thus, to a very good approximation, the extrapolation of the measured EMFs to zero buffer molality in Fig. 6 yields the EMF that the buffer would have if the activity coefficients γ_{TrisH^+} , γ_{Cl^-} , and γ_{Tris} were equal to their limiting values in the pure artificial seawater medium (generally referred to as trace activity coefficients).

Is a linear relationship between measured EMF and buffer molality at fixed salinity and temperature expected? The change in the activity coefficient contribution to the calculated EMF, from buffer molality $m(1)$ to molality $m(2)$, is given by:

$$\Delta E = - (RT/F) \left\{ \ln(\gamma_{\text{TrisH}^+} \gamma_{\text{Cl}^-} / \gamma_{\text{Tris}})_{m(2)} - \ln(\gamma_{\text{TrisH}^+} \gamma_{\text{Cl}^-} / \gamma_{\text{Tris}})_{m(1)} \right\} \quad (7)$$

Table 6Influence of interaction parameters and their differences on the change in EMF (ΔE) caused by a change in buffer molality 0.04 to 0.0 mol kg⁻¹ (salinity 35, and 25 °C).

Interaction	Parameters ^a	ΔE (mV) ^b
(TrisH ⁺ -Cl ⁻) - (Na ⁺ -Cl ⁻)	($\beta^{(0,1)}_{\text{TrisH,Cl}} - \beta^{(0,1)}_{\text{Na,Cl}}$), ($C^{(0,1)}_{\text{TrisH,Cl}} - C^{(0,1)}_{\text{Na,Cl}}$) ^c	0.124
Tris - Na ⁺	$\lambda_{\text{Tris,Na}}$	-0.0541
Tris self interactions	$\lambda_{\text{Tris,Tris}}$, $\mu_{\text{Tris,Tris,Tris}}$	-0.0105
(TrisH ⁺ - SO ₄ ²⁻) - (Na ⁺ -SO ₄ ²⁻)	($\beta^{(0,1)}_{\text{TrisH,SO}_4} - \beta^{(0,1)}_{\text{Na,SO}_4}$), ($C^{(0,1)}_{\text{TrisH,SO}_4} - C^{(0,1)}_{\text{Na,SO}_4}$) ^c	-0.0019
Known mixture parameters	$\Psi_{\text{Cl,SO}_4,\text{Na}}$, $\Psi_{\text{Na,Mg,Cl}}$, $\Psi_{\text{Na,Ca,Cl}}$, $\Psi_{\text{Na,K,Cl}}$	-0.00073

Notes: ΔE corresponds to the difference between the EMFs (indicated by the dashed line in Fig. 6) for buffer molalities of 0.04 and 0.0 mol kg⁻¹.^a The interaction parameters that influence ΔE are those listed above plus mixture parameters $\theta_{\text{Na,TrisH}}$, and ψ_{H^+} involving ions Na⁺ and Cl⁻, TrisH⁺ and Cl⁻, or Na⁺ and TrisH⁺.^b The sum of these calculated ΔE is 0.057 mV, which is less than the 0.15 mV obtained from the extrapolation of the measured EMFs (dotted line in Fig. 6).^c The individual parameter differences ($\beta^{(0)}_{\text{TrisH,Cl}} - \beta^{(0)}_{\text{Na,Cl}}$), ($\beta^{(1)}_{\text{TrisH,Cl}} - \beta^{(1)}_{\text{Na,Cl}}$), ($C^{(0)}_{\text{TrisH,Cl}} - C^{(0)}_{\text{Na,Cl}}$), and ($C^{(1)}_{\text{TrisH,Cl}} - C^{(1)}_{\text{Na,Cl}}$) on the first row; and the corresponding differences for TrisH⁺-SO₄²⁻ and Na⁺-SO₄²⁻ interactions on the fourth row.

where the two sets of activity coefficients will have different values at the two buffer molalities. Examination of the Pitzer model expressions for the combinations of the activity coefficient differences ($\ln(\gamma_{\text{TrisH}})_{m(2)} - \ln(\gamma_{\text{TrisH}})_{m(1)}$, etc.) shows that: (i) the contributions of the individual interaction parameters involving TrisH⁺ and Cl⁻ to the slope of the dashed line in Fig. 6 occur largely as the pairs ($\beta^{(0,1)}_{\text{TrisH,Cl}} - \beta^{(0,1)}_{\text{Na,Cl}}$), and ($C^{(0,1)}_{\text{TrisH,Cl}} - C^{(0,1)}_{\text{Na,Cl}}$). In the equations these are multiplied by factors in which the only varying quantity, at a fixed salinity, is m_{TrisH^+} (the molality of the added equimolar buffer). The same is true of most mixture parameters. This is why the dashed line in Fig. 6 is linear with respect to buffer molality. (ii) The influence of $\lambda_{\text{Tris,TrisH}}$ cancels in the equation above, and parameters for Tris-Tris and Tris-Na⁺ interactions occur only in the expression for γ_{Tris} .

The principal contributors to the calculated ΔE in Eq. (7), for $m(1)$ equal to 0.04 mol kg⁻¹ and $m(2)$ equal to 0 mol kg⁻¹, are listed in Table 6. There are very few, chiefly because the only change in the solution composition on the addition of buffer is the substitution of TrisH⁺ for Na⁺ and the addition of Tris. The molalities of the other seawater ions that are not pH dependent stay the same, as does the formal ionic strength. The largest interaction contribution is that of ((TrisH⁺-Cl⁻) - (Na⁺-Cl⁻)), followed by that for Tris-Na⁺. Future work to improve agreement between the measured and calculated EMFs of Tris buffer in artificial seawater, and the slope with respect to buffer molality, should focus on TrisH⁺-Cl⁻, TrisH⁺-Na⁺-Cl⁻ and Tris-Na⁺ interactions. It will be necessary to give particular attention to the differences between parameters involving TrisH⁺ and the corresponding ones for Na⁺, because it is these that directly contribute to ΔE in Eq. (7) and hence the slope of the dashed line in Fig. 6.

The activity coefficient term in Eq. (7), and its value for any given buffer molality $m(1)$ (with $m(2)$ equal to zero), represents the change in EMF caused by the presence of TrisH⁺ and Tris in the solution and the reduction in m_{Na^+} . The addition of this quantity to the measured EMF yields the EMF that this solution (containing buffer molality $m(1)$)

would have if the activity coefficients of TrisH⁺, Tris, and Cl⁻ were those characteristic of artificial seawater containing only trace quantities of TrisH⁺ and Tris. This is significant for several reasons. First, the presence of acid-base substances changes activity coefficients, such as those in Eq. (6), and it is important to allow for this when calculating properties of artificial seawater buffers. Second, the linear extrapolation of measured EMFs to zero buffer molality (in the absence of an accurate model) is reasonable, but the results in Fig. 6 suggest that data below about 0.02 mol kg⁻¹ buffer should not be included. We note that there is no visible deviation of the measured EMFs of DelValls and Dickson (1998) at 25 °C from linearity with respect to buffer molality, but there is some suggestion of this effect in the data for lower temperatures (not shown). Third, the slope of the modelled EMFs in Fig. 6 with respect to buffer molality (solid line, above about 0.02 mol kg⁻¹ of buffer) is slightly greater than that of the activity coefficient term (dashed line). However, the difference between the two, in terms of the estimated change in ($E - E^0$) between some buffer molality $m(1)$ and zero buffer molality is only about 0.02 to 0.03 mV. This is less than both the scatter in the data and the inherent uncertainty of the measurements. Consequently, as long as measured EMFs at low buffer molalities are excluded (below 0.02 mol kg⁻¹ according to the present model) they can be linearly extrapolated to zero buffer molality in order to obtain the EMF of a solution in which the activity coefficients are the same as they would be in pure artificial seawater, with very little added uncertainty.

5.4. The effect of varying molalities of TrisH⁺ and Tris relative to one another

Pratt (2014) has measured EMFs of artificial seawaters (of salinity 35) containing three different mole ratios of Tris buffer. At 25 °C the EMFs of the solutions containing the highest and lowest mole ratios (0.05:0.03, and 0.03:0.05 TrisH⁺:Tris) differ by about 26 mV, and the corresponding pH values range from 7.8521 to 8.2966 (table 3 of Pratt

Table 7

Measured and calculated EMFs of Tris buffer solutions of salinity 35 and 25 °C, for different buffer ratios.

$m_{\text{TrisH}^+}:m_{\text{Tris}}$	$-RT/F \cdot \ln(\gamma_{\text{TrisH}^+} \cdot \gamma_{\text{Cl}^-}/\gamma_{\text{Tris}})$ ^a (mV)	$-RT/F \cdot \ln(m_{\text{TrisH}^+}/m_{\text{Tris}})$ ^a (mV)	$E(\text{meas.})$ ^b (V)	$E(\text{calc.})$ ^c (V)	$E(\text{meas.}) - E(\text{calc.})$ (mV)
0.04:0.04	24.090	-0.01	0.73820 (± 0.000048)	-	-
0.05:0.03	24.097	-13.13	0.72498 (± 0.00055)	0.72508	-0.1
0.03:0.05	24.083	13.10	0.75127 (± 0.00012)	0.75131	-0.04

Notes

^a Calculated using the modified TrisH⁺-Cl⁻ parameters given in the notes to Table 2. These terms are from Eq. (6).^b Mean values (with standard deviations) of results of all cells for runs "Initial 298.15 K" listed in Tables S-1a to S-1c of the Supporting Information to Pratt (2014).^c This is the listed $E(\text{meas.})$ for the equimolar buffer plus the difference in the molality term in the previous column (the value for the buffer ratio of interest, minus the value for the equimolar buffer). The activity coefficient term, which varies by less than 0.01 mV relative to the value for the equimolar buffer, is neglected in this calculation. See Eq. (6).

(2014)). The EMFs of these buffer solutions can be calculated with Eq. (6). The only contributions that vary, for differing ratios of buffer substances in a constant salinity medium, are the activity coefficient term ($\ln(\gamma_{\text{TrisH}^+}\gamma_{\text{Cl}^-}/\gamma_{\text{Tris}})$) and the molality term ($\ln(m_{\text{TrisH}^+}/m_{\text{Tris}})$). Their calculated values are listed in Table 7 for the three solutions measured. The results show that the contribution of the activity term to the EMF is expected to change by only ± 0.007 mV relative to its value for the equimolar buffer solution. We also calculate that, for all three solutions, the molalities of the TrisH^+ and Tris in the solutions remain almost unaltered from their stoichiometric nominal values (given in the first column of Table 7). Consequently, the difference in the EMF between two artificial seawater solutions at the same salinity and temperature, and containing two different buffer ratios R(1) and R(2) but the same total amount of added Tris ($m_{\text{Tris}} + m_{\text{TrisHCl}}$), can be calculated from:

$$E_{R(2)} = E_{R(1)} + (RT/F) \left\{ \ln(m_{\text{TrisH}^+}/m_{\text{Tris}})_{R(1)} - \ln(m_{\text{TrisH}^+}/m_{\text{Tris}})_{R(2)} \right\} \quad (8)$$

where the two subscripts indicate that the values (EMFs, or molality quotients) are for the two buffer ratios of interest. This equation implies that, at a fixed salinity and temperature, the quantity $[E + (RT/F) \cdot \ln(m_{\text{TrisH}^+}/m_{\text{Tris}})]$ is constant. Deviations of the measurements of Pratt (2014) from this simple relationship are plotted in Fig. 7, as the quantity δE , and are shown to be within the uncertainties of the measurements. The additional contribution of the deviations of the $m_{\text{TrisH}^+}/m_{\text{Tris}}$ ratio from the nominal value (due to the shifting chemical equilibrium, and calculated using the model) is plotted as a solid line in the figure, and is very small (< 0.02 mV).

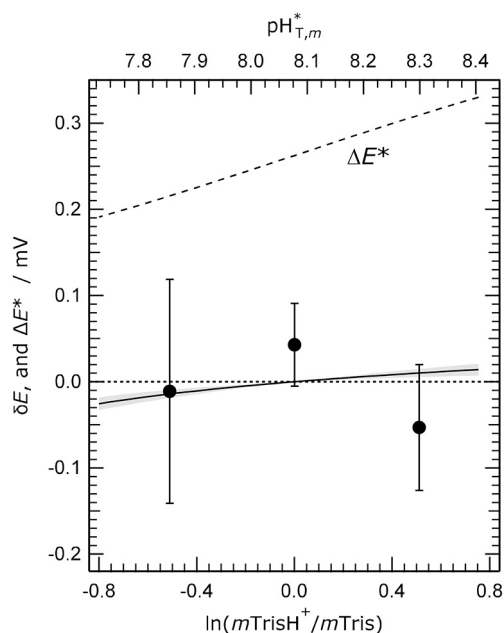


Fig. 7. EMFs measured by Pratt (2014) (at 25 °C, in artificial seawater of salinity 35) for three different $\text{TrisH}^+:\text{Tris}$ ratios, compared with values calculated using Eq. (8). Symbols (δE): deviations of $[E + (RT/F) \cdot \ln(m_{\text{TrisH}^+}/m_{\text{Tris}})]$ from a weighted mean of the values for the three buffer ratios. Quantity E (V) is the measured EMF and molalities m_{TrisH^+} and m_{Tris} are the stoichiometric values in the solutions as prepared (i.e., assuming complete neutralisation of Tris by the smaller added molality of HCl, to yield TrisH^+). The error bars indicate the standard deviations of the measured EMFs. Lines: solid – the model-calculated effect of the change in m_{TrisH^+} and m_{Tris} from the stoichiometric values, together with the envelope of computed uncertainties (< 0.01 mV at the extremes of the plot); dashed – the calculated difference term (ΔE^* , Eq. (14) in Section 6) present in the definition of total pH. The upper horizontal axis shows the calculated pH ($\text{pH}^*_{T,m}$) that corresponds to the $m_{\text{TrisH}^+}/m_{\text{Tris}}$ ratios on the lower x-axis, centered on a defined 8.0772 for the 1:1 ratio.

Equation (8) should be helpful both in adjusting buffer pH for known (unintended) imbalances between m_{TrisH^+} and m_{Tris} , and for the preparation of buffers with a higher or lower pH than that normally used. The relationship between EMF (and consequently pH) and the ratio $m_{\text{TrisH}^+}/m_{\text{Tris}}$, embodied in Eqs. (6) and (8) above, is essentially equivalent to the Henderson-Hasselbalch relationship used by Pratt (2014) (see his eq. (8)).

6. The pH of Tris buffers in artificial seawater on the total scale

In this section we clarify the algebraic relationships between the EMFs of Harned cells that contain Tris buffers in artificial seawater, the conventional thermodynamic total molality ($m_{\text{H}^+} + m_{\text{HSO}_4^-}$), and two alternate approaches to assigning so-called total hydrogen ion molalities which are the basis of the total pH scale for seawater. These approaches are:

- (1) The formal total hydrogen molality, $(m_{\text{H}^+}^{\text{(T)}})_f$, originally described by Dickson (1984) and subsequently defined more rigorously by Dickson (1990) and DelValls and Dickson (1998). This is a close approximation to $(m_{\text{H}^+} + m_{\text{HSO}_4^-})$ in a Tris buffer.
- (2) The operational total hydrogen ion molality, $m_{\text{H}^+}^{\text{(T)}}$, described by DelValls and Dickson (1998) and intended as an approximation to $(m_{\text{H}^+}^{\text{(T)}})_f$ in a Tris buffer. It is this operational total hydrogen ion molality that, after conversion to a mol kg^{-1} of seawater basis, calibrates the seawater total pH scale (e.g., eq. (18) of DelValls and Dickson (1998) which gives the operational total pH of a Tris buffer as a function of temperature and salinity).

The equivalent pH to the above measures of total hydrogen ion concentration are, in the same order: $\text{pH}^*_{T,m}$ (equal to $-\log_{10}(m_{\text{H}^+} + m_{\text{SO}_4^{2-}})$), $(\text{pH}_{T,m})_f$ (equal to $-\log_{10}((m_{\text{H}^+}^{\text{(T)}})_f)$), and $\text{pH}_{T,m}$ (equal to $-\log_{10}(m_{\text{H}^+}^{\text{(T)}})$). In this section we also determine the uncertainty contributions of equilibrium constants and individual Pitzer parameters to modelled values of pH (or EMF) to identify those terms that are the most important for accurate predictions of buffer solution properties. The model is used to quantify the difference between the three measures of total hydrogen ion molality, for Tris buffers made up in artificial seawaters of varying salinity and from equimolar amounts of the buffer species m_{Tris} and m_{TrisH^+} . We also illustrate the relationship between these three quantities, and their extrapolations to zero added buffer molality, in artificial seawater of salinity 35. All measures of pH discussed in this section are on a molality basis, indicated by the subscript m , reflecting the explicit use of molality in the Pitzer model and other thermodynamic speciation models for aqueous solutions. Conversions to a mol kg^{-1} of seawater (amount content) basis, the common usage in marine chemistry, are given in the Appendix. The different measures of pH used in this work are summarised in Chart I (see also the Glossary of Symbols).

6.1. Total pH and the EMFs of Tris buffers in artificial seawater

The operational total pH scale is calibrated using Harned cell measurements of buffer solutions in artificial seawater, made up with equimolar quantities of TrisH^+ and Tris (DelValls and Dickson, 1998), combined with a standard cell potential determined from measurements of acidified artificial seawater extrapolated to zero added HCl (Dickson, 1990, see his eq. (14)). Values of $-\log_{10}(m_{\text{H}^+}^{\text{(T)}})$ obtained in this way will be close, but not identical, to $-\log_{10}(m_{\text{H}^+} + m_{\text{HSO}_4^-})$ and $(m_{\text{H}^+}^{\text{(T)}})_f$ in the Tris buffer solutions.

First, we repeat the derivation from paper (I) of the expression for the Harned cell standard EMFs of artificial seawaters used in the definition of total pH. We begin by defining a conventional thermodynamic total hydrogen ion molality, for any solution, as the sum of the free hydrogen ion molality (m_{H^+}) and the bisulphate molality ($m_{\text{HSO}_4^-}$):

$$m\text{H}^+ + m\text{HSO}_4^- = m\text{H}^+ (1 + m\text{SO}_4^{2-}/K^*(\text{HSO}_4^-)) \quad (9)$$

where $m\text{SO}_4^{2-}$ is the molality of the free sulphate in solution, and $K^*(\text{HSO}_4^-)$ is the stoichiometric dissociation constant of the bisulphate ion given by:

$$K^*(\text{HSO}_4^-) = m\text{H}^+ \cdot m\text{SO}_4^{2-} / m\text{HSO}_4^- = K(\text{HSO}_4^-) \cdot (\gamma_{\text{HSO}_4^-} / \gamma_{\text{H}^+} \cdot \gamma_{\text{SO}_4^{2-}}) \quad (10)$$

In this equation $K(\text{HSO}_4^-)$ is the thermodynamic value of the dissociation constant at the temperature of interest. The three activity coefficients all vary with temperature and the composition of the solution (variations with pressure are not considered in this work).

The EMF of a Harned cell, containing a solution with H^+ and Cl^- ions, can be expressed in terms of the conventional thermodynamic total hydrogen ion molality as follows:

$$E = \{E^0 - (RT/F) \cdot [2\ln(\gamma_{\text{HCl}}) - \ln(1 + m\text{SO}_4^{2-}/K^*(\text{HSO}_4^-))] \} - (RT/F) \cdot \ln((m\text{H}^+ + m\text{HSO}_4^-) \cdot m\text{Cl}^-) \quad (11)$$

where γ_{HCl} is the mean activity coefficient of HCl in the solution. If Eq. (11) is applied to solutions not containing SO_4^{2-} , then $m\text{HSO}_4^-$ and the logarithmic term including $m\text{SO}_4^{2-}$ on the first line will both be zero. For a solution of artificial seawater containing added HCl, the limiting value of the quantity in $\{\}$ in Eq. (11) as the amount of HCl tends to zero is equivalent to a standard potential of the cell (E^*) for the temperature and salinity of interest. It is obtained experimentally from measurements of a series of such solutions containing differing molalities of HCl (Dickson, 1990). Thus:

$$E^* = E^0 - (RT/F) \cdot [2\ln(\gamma_{\text{HCl}}^{(\text{tr})}) - \ln(1 + m\text{SO}_4^{2-(\text{T})}/K^*(\text{HSO}_4^-)^{(\text{tr})})] \quad (12)$$

where the superscript (tr) indicates the limiting value of the term in pure artificial seawater (i.e., as the added amount of HCl tends to zero). (See the Appendix for an explanation of the meaning of *trace* in both practical and modelling contexts.) At this hypothetical limit the molality of HSO_4^- is so small that $m\text{SO}_4^{2-}$ becomes the total SO_4^{2-} molality, denoted by superscript (T). This definition is eq. (13) of Dickson (1990).

Values of E^* were obtained by Dickson (1990) from measurements of EMFs in artificial seawater, acidified with 0.0025 to 0.0379 mol kg^{-1} HCl. The extrapolation to zero added HCl was achieved using a quadratic fit of the quantity given in the second part of his Eq. (13). Although model-calculated EMFs of acidified artificial seawater were found to deviate from measured values, our results in paper (I) confirm that the procedure used by Dickson (1990) to obtain E^* yields values that correspond to the definition in Eq. (12). The equation for E^* given by Dickson (1990) has a goodness of fit of 0.024 mV, comparable to the typical standard uncertainty of Harned cell EMF measurements of about 0.04 mV (see document 6 of the Supporting Information).

The standard EMF, E^* , defined by Eq. (12) and determined by an extrapolation in terms of total H^+ ion molality, can be used to interpret buffer solution EMFs expressed on the same total H^+ basis. Thus, substituting for E^0 (from Eq. (12) into Eq. (11)), we obtain for the general case:

$$E = E^* - (RT/F) \cdot \ln((m\text{H}^+ + m\text{HSO}_4^-) \cdot m\text{Cl}^-) - (RT/F) \cdot 2\ln(\gamma_{\text{HCl}}/\gamma_{\text{HCl}}^{(\text{tr})}) + (RT/F) \cdot \ln\left[\frac{(1 + m\text{SO}_4^{2-}/K^*(\text{HSO}_4^-))}{(1 + m\text{SO}_4^{2-(\text{T})}/K^*(\text{HSO}_4^-)^{(\text{tr})})}\right] \quad (13)$$

where γ_{HCl} is the mean activity coefficient of HCl, $K^*(\text{HSO}_4^-)$ is the stoichiometric dissociation constant of HSO_4^- , and $m\text{SO}_4^{2-}$ is the free sulphate molality, all in the solution of interest. The quantities $\gamma_{\text{HCl}}^{(\text{tr})}$, $m\text{SO}_4^{2-(\text{T})}$, and $K^*(\text{HSO}_4^-)^{(\text{tr})}$ have the same meanings as in Eq. (12). The final two logarithmic terms in Eq. (13) represent the EMF change caused by the change in composition between the solution of interest and the original artificial seawater composition for which E^* was determined.

Henceforth we will refer to the sum of these quantities as the E^* difference term, ΔE^* , defined by:

$$\Delta E^* = -(RT/F) \cdot 2\ln(\gamma_{\text{HCl}}/\gamma_{\text{HCl}}^{(\text{tr})}) + (RT/F) \cdot \ln\left[\frac{(1 + m\text{SO}_4^{2-}/K^*(\text{HSO}_4^-))}{(1 + m\text{SO}_4^{2-(\text{T})}/K^*(\text{HSO}_4^-)^{(\text{tr})})}\right] \quad (14)$$

Eq. (13) differs from eq. (7) of DelValls and Dickson (1998) in that they substituted their eq. (5) for E^* (which is the same as eq. (13) of Dickson (1990) and our Eq. (12)) into the expression for cell EMF on a free H^+ basis. This is a consequence of the decision of Dickson (1990) to define the formal total hydrogen ion molality so that it remains proportional to the free hydrogen ion molality at all pH (at a fixed salinity and temperature). This is equivalent to assuming that the value of $(1 + m\text{SO}_4^{2-}/K^*(\text{HSO}_4^-))$ in the buffer or other solution is identical to its limiting value in artificial seawater, thus making the final logarithmic term in Eqs. (13) and (14) above equal to zero.

In Tris buffer solutions at salinities and temperatures corresponding to E^* , the value of $\gamma_{\text{HCl}}/\gamma_{\text{HCl}}^{(\text{tr})}$ in Eqs. (13) and (14) will be close to unity, and $K^*(\text{HSO}_4^-)$ will be close to $K^*(\text{HSO}_4^-)^{(\text{tr})}$. The small differences are caused by the presence of the Tris, and the TrisH^+ (which is substituted for Na^+). Furthermore, in the buffer solution the molality of HSO_4^- is very much less than that of SO_4^{2-} and therefore $m\text{SO}_4^{2-}$ in eq. (13) is effectively the same as $m\text{SO}_4^{2-(\text{T})}$. Thus, both the final two terms in Eq. (13) are likely to be small, although increasing at lower salinities as the molalities of the buffer substances become larger relative to those of the seawater components. The values of the quantities in these last two terms, i.e. ΔE^* , cannot be determined experimentally.

6.2. Model calculations of $(m\text{H}^+ + m\text{HSO}_4^-)$, and $m\text{H}^+$

It is desirable that speciation models be able to calculate accurately both $m\text{H}^+$ and $m\text{HSO}_4^-$ in Tris buffer solutions in order to quantify ΔE^* and therefore relate the operationally determined value of $m\text{H}^{+(\text{T})}$ in such buffers to $(m\text{H}^+ + m\text{HSO}_4^-)$ and $(m\text{H}^{+(\text{T})})_f$, and also to make progress in a number of pH related areas: the extension of the total pH scale to low salinities, establishing a relationship between the total scale and other scales, and quantifying the effects of composition changes relative to seawater stoichiometry (hence the preparation of buffers relevant to other natural waters). We have therefore determined uncertainty profiles for both $-\log_{10}(m\text{H}^+ + m\text{HSO}_4^-)$ ($\text{pH}^*_{\text{T},m}$) and $-\log_{10}(m\text{H}^+)$ ($\text{pH}^*_{\text{F},m}$, for the conventional thermodynamic free H^+ molality) in 0.04 mol kg^{-1} equimolar Tris H^+ /Tris in seawater of salinity 35, at 25 °C. Two sets of calculations were carried out: (i) with the variances of interaction parameters whose values are unknown set to zero, and with variances of parameters $\lambda_{\text{Tris},M}$ (where M is a metal cation) set to values estimated by simulation; (ii) using averaged values and associated variances, from Appendix A of paper (I), for parameters whose values are unknown, and with variances of parameters $\lambda_{\text{Tris},M}$ set to the squares of the standard deviations determined by fitting (Table 2).

The results of the first group of calculations are shown in Fig. 8. Comparing the uncertainty profile for $\text{pH}^*_{\text{T},m}$ (Fig. 8a) with the corresponding one for the calculated EMF (Fig. 2), it is clear that $\ln(K(\text{HSO}_4^-))$ and H^+ - Cl^- interactions become very important contributors to the variance in calculated $\text{pH}^*_{\text{T},m}$, accounting for about 60% of the total compared to about 22% for Tris H^+ - Cl^- interactions (which contribute about 70% to the variance in the calculated EMF). This is for two reasons: first, although the H^+ activity is determined by $K(\text{TrisH}^+)$ and the Tris H^+ and Tris activities, the molality of H^+ depends on its activity coefficient which is largely controlled by the interaction with Cl^- . The uncertainty in the molality of HSO_4^- , which is also an element of $\text{pH}^*_{\text{T},m}$, is largely due to that in $K(\text{HSO}_4^-)$. Of the parameter group $(\theta_{\text{Cl},\text{SO}_4}, \psi_{\text{Cl},\text{SO}_4,\text{Na}}, \psi_{\text{Cl},\text{SO}_4,\text{Mg}})$ in Fig. 8(a), the variance contribution of $\theta_{\text{Cl},\text{SO}_4}$ exceeds that of $\psi_{\text{Cl},\text{SO}_4,\text{Na}}$ by a factor of about 30, and that of $\psi_{\text{Cl},\text{SO}_4,\text{Mg}}$ by more than 100. There are a large number of parameter

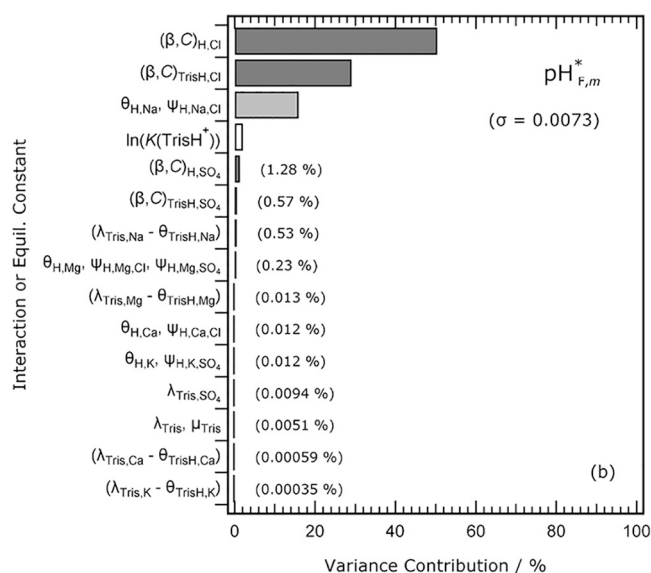
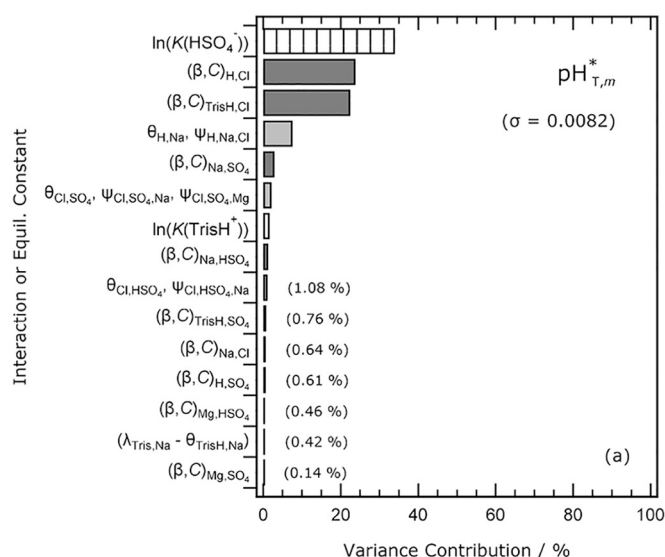


Fig. 8. Percentage contributions of individual Pitzer model interactions, and equilibrium constants, to the variance of the calculated $\text{pH}^*_{\text{T},m}$ (panel a), and $\text{pH}^*_{\text{F},m}$ (panel b), of a 0.04 mol kg^{-1} equimolar $\text{TrisH}^+/\text{Tris}$ buffer in a salinity 35 artificial seawater at 25°C . The parameters associated with each of the interactions are listed down the left-hand sides, and contributions of about 1% and below are noted on the plots. Interactions with very small variance contributions are omitted. In these calculations the variances of all unknown parameters are set to zero, and those of the Tris-metal cation interaction parameters are simulated values. Only the top 15 contributions are listed. The standard uncertainty of the calculated pH value is noted on each plot.

groups that only contribute to the total variance at or below the 1–2% level.

The HSO_4^- ion does not contribute to $\text{pH}^*_{\text{F},m}$, which eliminates $\ln(K(\text{HSO}_4^-))$ and all interaction parameters involving this anion from the uncertainty profile in Fig. 8b. This profile is notably simpler than that for $\text{pH}^*_{\text{T},m}$, and there are only five variance contributions above 1%. The H^+-Cl^- and $\text{TrisH}^+-\text{Cl}^-$ interactions together account for almost 80% of the total variance in the calculated $\text{pH}^*_{\text{F},m}$. The ternary interactions $\text{H}^+-\text{Na}^+-\text{Cl}^-$ are also important (contributing about 15% of the total variance).

The second set of calculations of $\text{pH}^*_{\text{T},m}$ and $\text{pH}^*_{\text{F},m}$, referred to above, are shown in Fig. 9. For $\text{pH}^*_{\text{T},m}$ the changes are small, and consist of contributions of about 2% from the unknown $\text{TrisH}^+-\text{HSO}_4^-$ interaction, and about 1% for both $(\theta_{\text{H,TrisH}}, \psi_{\text{H,TrisH,Cl}})$ and $(\lambda_{\text{Tris,Mg}} - \theta_{\text{TrisH,Mg}})$. In the

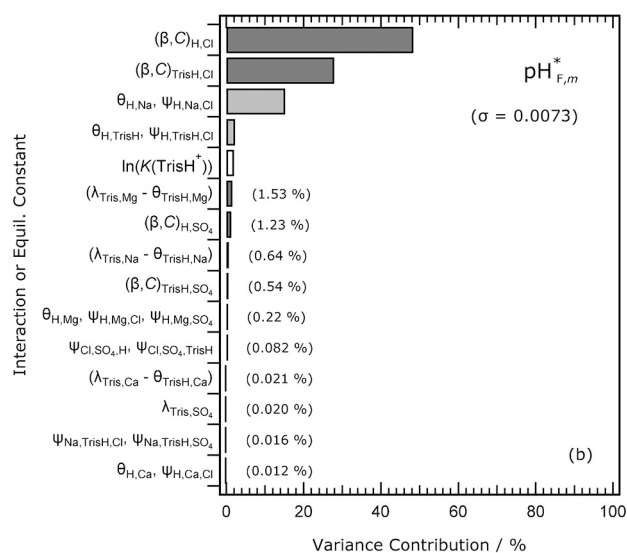
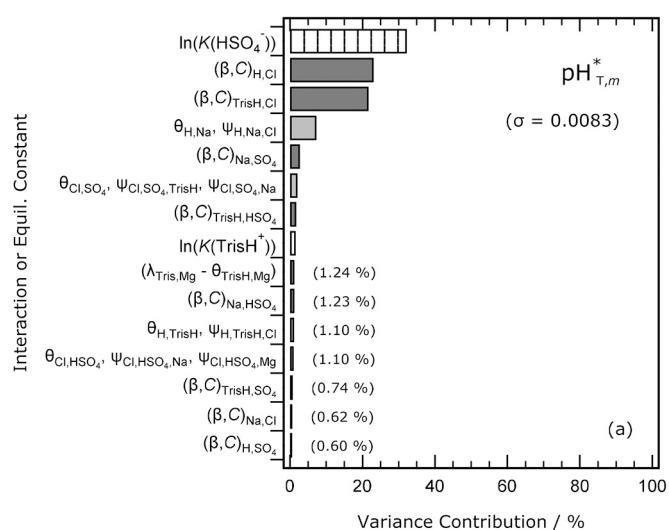


Fig. 9. Percentage contributions of individual Pitzer model interactions, and equilibrium constants, to the variance of the calculated $\text{pH}^*_{\text{T},m}$ (panel a), and $\text{pH}^*_{\text{F},m}$ (panel b), of a 0.04 mol kg^{-1} equimolar $\text{TrisH}^+/\text{Tris}$ buffer in a salinity 35 artificial seawater at 25°C . These calculations are the same as in Fig. 8, except: (i) the values and variances of all unknown parameters are set to averaged values listed in the tables in Appendix A to paper (I); (ii) the variances of the Tris-metal cation interaction parameters $\lambda_{\text{Tris,M}}$ (where M is the metal cation) were set to the squares of the standard deviations from the fits described in Section 2. These are generally larger than the simulated variances (with the exception of that for $\lambda_{\text{Tris,Na}}$).

latter case this is because the fitted value (see Fig. 1) has a large standard deviation. For the uncertainty profile of $\text{pH}^*_{\text{F},m}$ shown in Fig. 9b the only significant changes relative to the base case in Fig. 8b are the contributions of $(\theta_{\text{H,TrisH}}, \psi_{\text{H,TrisH,Cl}})$ at about 2% of the calculated variance, and about 1.5% for $(\lambda_{\text{Tris,Mg}} - \theta_{\text{TrisH,Mg}})$ for the same reasons noted above.

These uncertainty profiles of $\text{pH}^*_{\text{T},m}$ and $\text{pH}^*_{\text{F},m}$ show that no additional interaction parameters are important contributors to the total variances of these quantities in the buffer solution beyond those already identified for the calculation of EMFs of acidified artificial seawater, Tris buffer in artificial seawater, and the quantity ΔE^* .

6.3. The relationship between pH on the total scale and $(m\text{H}^+ + m\text{HSO}_4^-)$

The total pH of a Tris buffer on a molality basis, $\text{pH}_{\text{T},m}$, is operationally calibrated from measured EMFs of the buffer solutions according to the following equations:

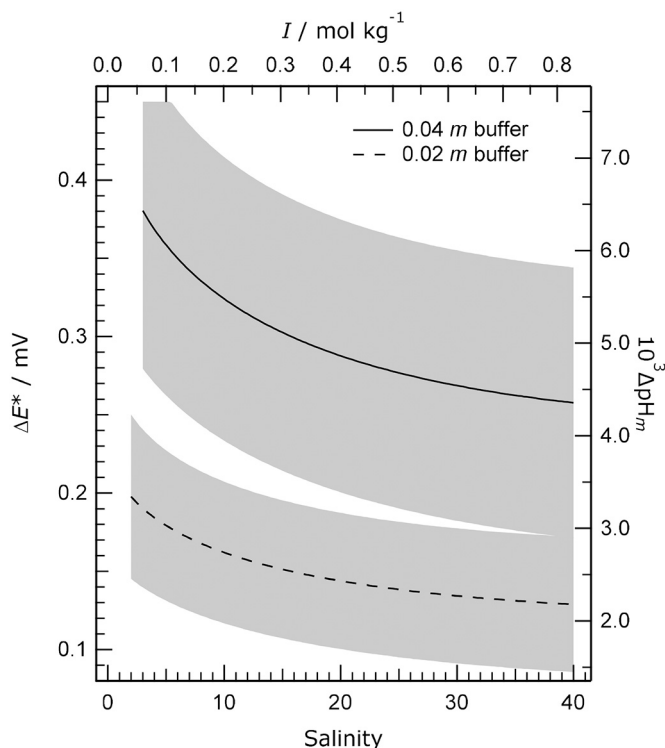


Fig. 10. Calculated values of the difference term in the standard EMF (ΔE^* , defined in Eq. (14)) at 25 °C, for two different TrisH⁺/Tris buffer molalities at various salinities. Lines: solid – 0.04 mol kg⁻¹ equimolal TrisH⁺/Tris; dashed – 0.02 mol kg⁻¹ equimolal TrisH⁺/Tris. The calculated standard uncertainties are shown as shaded areas around each line. The top axis indicates the ionic strength of the artificial seawater that corresponds to the indicated salinities (bottom axis). The right-hand axis shows ΔE^* , but in equivalent molality-based pH units (equal to $\Delta E^* \cdot F / (RT \cdot \ln(10))$).

$$-\ln(mH^{+(T)}) = (F/RT)(E - E^*) + \ln(mCl^-) \quad (15a)$$

$$pH_{T,m} = -\log_{10}(mH^{+(T)}) \quad (15b)$$

where $mH^{+(T)}$ is the operational total hydrogen ion molality assigned to the particular buffer, E is the measured EMF of the Tris buffer solution, and E^* is the standard EMF of the cell (Eq. (12)). Comparison of Eqs. (15a) and (13) shows that $mH^{+(T)}$ and the conventional thermodynamic total ($mH^+ + mHSO_4^-$) in an aqueous solution are related by:

$$\ln(mH^{+(T)}) = \ln(mH^+ + mHSO_4^-) + 2\ln(\gamma_{HCl}/\gamma_{HCl}^{(tr)}) - \ln\left[\frac{(1 + mSO_4^{2-}/K^*(HSO_4^-))}{(1 + mSO_4^{2-(T)}/K^*(HSO_4^-)^{(tr)})}\right] \quad (16a)$$

$$= \ln(mH^+ + mHSO_4^-) - (F/RT) \cdot \Delta E^* \quad (16b)$$

We have used the present model to estimate the values of the last two terms in Eq. (16a) for an artificial seawater of salinity 35, and equimolal Tris buffer (containing 0.04 mol kg⁻¹ of Tris and TrisH⁺) at the same salinity, both at 25 °C. The revised TrisH⁺-Cl⁻ parameters (given in the notes to Table 2) were used. We obtain -0.0071 for the contribution of the activity coefficient term in Eq. (16a) and -0.0045 for the term containing the bisulphate dissociation constants. (Note that all quantities are in natural logarithms.) These are equivalent to a combined factor of 1.012 by which $mH^{+(T)}$ should be multiplied to obtain ($mH^+ + mHSO_4^-$) in the buffer. The two contributions to ΔE^* (Eq. (14)) for these solutions are 0.18 mV for the activity coefficient term, and 0.112 mV for the bisulphate term. Both are linearly dependent upon the buffer molality (at a fixed salinity), so that as the buffer molality tends to zero the values of the two terms also tend to zero.

A second set of calculations, in which unknown interaction parameters were assigned averaged values from Table A1 from Appendix A of paper (I), yielded 0.26 mV for ΔE^* at salinity 35, which is slightly less than for the base case. Figure 10 shows ΔE^* at 25 °C for two buffer molalities over a wide salinity range (calculated using the same set of interaction parameters). The important features of this result are: first, values of ΔE^* for the 0.02 mol kg⁻¹ buffer are half those for the 0.04 mol kg⁻¹ buffer. Second, even at a salinity of 5 the value of ΔE^* for the 0.04 mol kg⁻¹ buffer has only increased by about 50% compared to the value of 40 salinity. This suggests that the total pH scale could readily be

Table 8

Measured and calculated quantities for 0.04 mol kg⁻¹ equimolal Tris buffer in artificial seawater of salinity 35 at 25 °C.

Quantity	Measured	Calculated (standard model)		Calculated (revised TrisH ⁺ -Cl ⁻ parameters)	
		std. $K(HSO_4^-)^a$	mod. $K(HSO_4^-)^b$	std. $K(HSO_4^-)^a$	mod. $K(HSO_4^-)^b$
$E - E^0$ (V)	0.51620 ^c ($\pm 3.1 \times 10^{-5}$)	0.51548 ($\pm 2.8 \times 10^{-4}$)	same as for std. value ^d	0.51609	same as for std. value ^d
$pH_{T,m}$	8.077 ^e ($\pm 7.1 \times 10^{-4}$)	8.0615 ^f (± 0.0095)	8.065 ^f (± 0.0095)	8.072 ^f	8.075 ^f
$-\log_{10}(mH^+ + mHSO_4^-)$, or $pH_{T,m}^*$	8.073 ^g (± 0.0016)	8.057 ^h (± 0.0082)	8.060 ^h (± 0.0082)	8.067 ^h	8.070 ^h
$-\log_{10}(mH^+)$, or $pH_{T,m}^*$	8.180 ⁱ	8.169 ^h (± 0.0073)	same as for std. value ^d	8.179 ^h	same as for std. value ^d

Notes: No uncertainties are listed for values calculated using the revised TrisH⁺-Cl⁻ Pitzer interaction parameters determined in this work because of the partial inconsistencies of the two datasets upon which they are based (which have yet to be resolved).

^a Calculated using the standard value of $K(HSO_4^-)$ in the model of Waters and Millero (2013) (from Clegg et al., 1994).

^b Calculated using the modified $K(HSO_4^-)$, from eq. (6) of Dickson et al. (1990).

^c The value of E^0 is taken to be 0.22240 V, the data are from table 2 of DelValls and Dickson (1998) and the uncertainty is the standard deviation of the 16 measured values.

^d This calculated quantity is independent of the value of $K(HSO_4^-)$.

^e The measurement-based value was calculated from eq. (18) of DelValls and Dickson (1998) (converted to a molality basis), and uncertainty is the goodness of fit statistic of that equation.

^f This calculated value includes the influence of the ΔE^* term given by Eq. (14), and its uncertainty.

^g Converted from the measurement-based $pH_{T,m}$ above using ΔE^* calculated by the model.

^h Calculated directly, using the model.

ⁱ Converted from the 8.073 for $-\log_{10}(mH^+ + mHSO_4^-)$ above, and using $K^*(HSO_4^-)$ from eq. (23) of Dickson (1990). No uncertainty is stated because, (i) the determination of $K^*(HSO_4^-)$ was dependent upon model-calculated γ_{HCl} in the acidified seawater solutions, and (ii) the value of $K^*(HSO_4^-)$ is for pure artificial seawater and not the buffer solution. It is expected that the overall uncertainty in $-\log_{10}(mH^+)$ is similar to, or greater than, that for $-\log_{10}(mH^+ + mHSO_4^-)$ above.

extended below the current lower limit of salinity 20 using the experimental approach of DelValls and Dickson (1998) unchanged. For a buffer molality of 0.02 mol kg^{-1} a salinity of 2 could be attained, because of the reduced amount of TrisH^+ that substitutes for Na^+ . Third, the calculated uncertainty envelope, for the 0.04 mol kg^{-1} buffer, is about $\pm 0.1 \text{ mV}$. It seems likely that relatively modest improvements in the model would enable this to be reduced to close to the roughly $\pm 0.04 \text{ mV}$ uncertainty of the Harned cell measurements on which the total pH scale is based. This would facilitate conversions between measured $\text{pH}_{T,m}$ and the conventional ($m\text{H}^+ + m\text{HSO}_4^-$) needed for general speciation calculations.

Measured and calculated ($E - E^0$) are compared in Table 8 for 0.04 mol kg^{-1} equimolar Tris buffer in salinity 35 seawater. The EMF of the buffer solution predicted using the revised $\text{TrisH}^+\text{-Cl}^-$ parameters (0.51609 V) differs from the experimental value by only 0.11 mV , which is close to the average for the data at all salinities given in Section 5.2 (0.13 mV). Values of $\text{pH}_{T,m}$ from measurements are also compared in Table 8 with estimates determined using the model (after adjustment for the influence of ΔE^*). There is a difference of $0.016 \text{ pH}_{T,m}$ units, using the model in its standard form. However, with the revised $\text{TrisH}^+\text{-Cl}^-$ interaction parameters and $K(\text{HSO}_4^-)$ from Dickson et al. (1990) this

difference is reduced to -0.002 units which gives confidence that revisions to the model can increase its accuracy substantially. Further comparisons in Table 8, in terms of $-\log_{10}(m\text{H}^+ + m\text{HSO}_4^-)$, in which the measurement-based value is obtained by subtracting the influence of ΔE^* from $\text{pH}_{T,m}$, show a similar picture. For $\text{pH}_{F,m}^*$ ($-\log_{10}(m\text{H}^+)$) the measurement-based value (8.180) and that calculated using the model with revised $\text{TrisH}^+\text{-Cl}^-$ parameters (8.179) differ by less than the uncertainty that arises from the measurement of EMF in the buffer solution and the determination of $K^*(\text{HSO}_4^-)$. We note that both buffer EMF, and values of $m\text{H}^+$ in the buffer solutions, are insensitive to HSO_4^- formation for reasons given previously and are therefore unaffected by the value of $K(\text{HSO}_4^-)$ used in the model.

In order to determine which interaction parameters in the model contribute most to the uncertainties in ΔE^* we have calculated uncertainty profiles for ΔE^* of 0.04 mol kg^{-1} buffer in artificial seawaters of salinities 5 to 35, see Fig. 11. Only the ten largest variance contributions are shown. Recall that the quantities of interest in Eq. (14) are γ_{H} , $\gamma_{\text{HSO}_4^-}$, γ_{SO_4} and γ_{Cl} in the two solutions. It is important to assess the possible influence of unknown interaction parameters – particularly those involving HSO_4^- for which relatively few are known. To achieve this, the unknown Pitzer interaction parameters were assigned averaged values

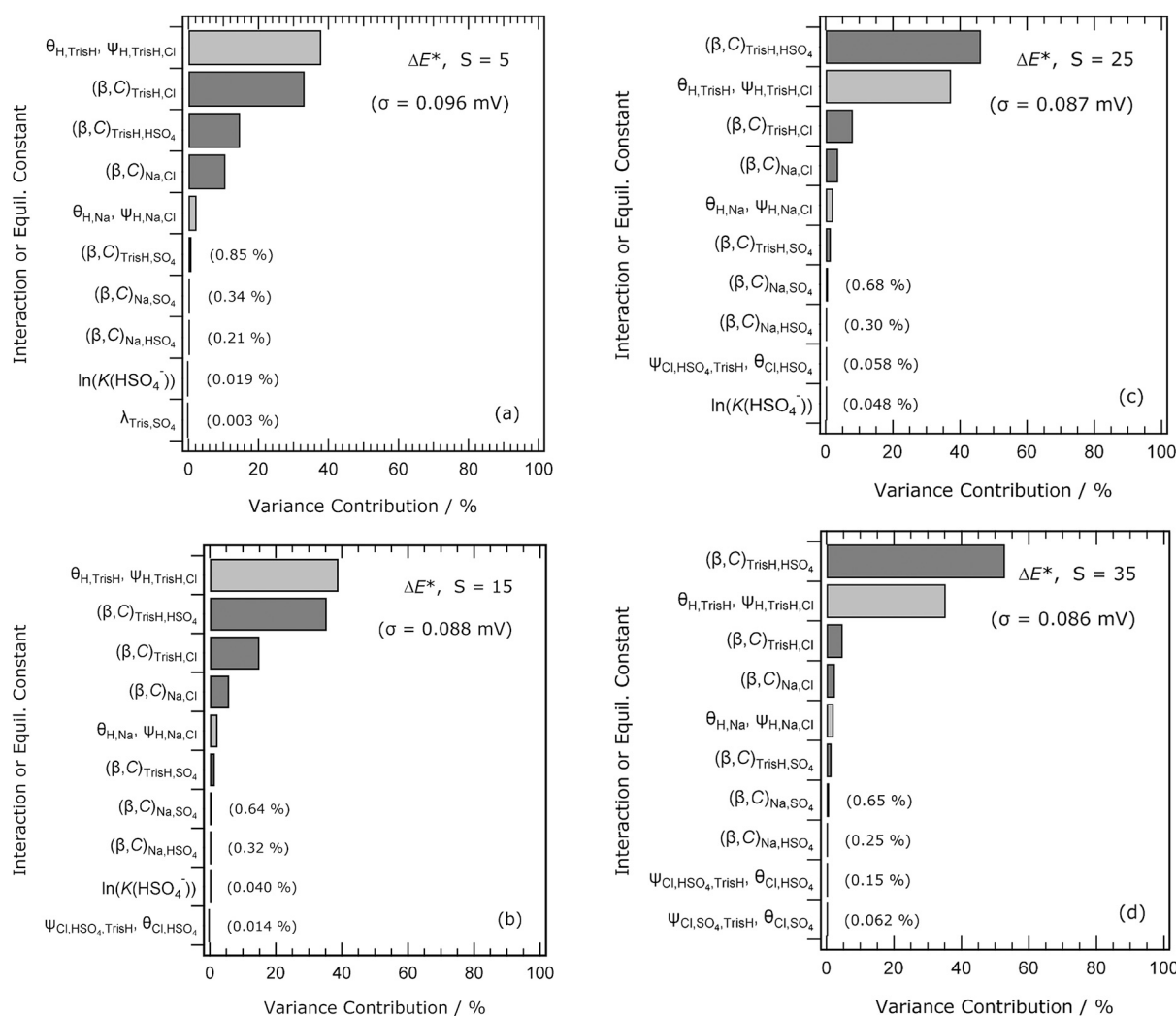


Fig. 11. Percentage contributions of individual Pitzer model interactions and equilibrium constants to the variance of the calculated difference term in the standard EMF (ΔE^* , defined in Eq. (14)) at 25°C , for 0.04 mol kg^{-1} equimolar TrisH^+ /Tris buffer in artificial seawater at four different salinities S (indicated on the plots). The parameters associated with each of the interactions are listed down the left-hand side, and contributions of $<1\%$ are noted on the plot. Interactions with very small variance contributions are omitted. In plots (b) and (c) the variance contribution of $\psi_{\text{Cl,HSO}_4,\text{Na}}$ is similar in magnitude to that of $\theta_{\text{Cl,HSO}_4}$ (and it is in the same group of interactions), but it is not shown. In plot (d) the same applies to parameters $\psi_{\text{Cl,HSO}_4,\text{Na}}$ and $\psi_{\text{Cl,SO}_4,\text{Na}}$ in the bottom two groups. The standard uncertainties of the calculated ΔE^* are noted on the plots.

from Appendix A of paper (I), and variances set equal to the squares of the listed standard deviations. Parameters $\theta_{\text{TrisH},M}$ and $\psi_{\text{TrisH},M,\text{Cl}}$ for metal cations M were set to zero for the reasons described in Section 5.1. The cation-cation parameters $\theta_{\text{TrisH},M}$ have no influence on the four activity coefficients appearing in the above expressions, and therefore would not appear in the uncertainty profiles in Fig. 11. Regarding $\psi_{\text{TrisH},M,\text{Cl}}$ we note that the analogous parameters $\psi_{\text{TrisH},M,\text{SO}_4}$ only make contributions to the calculated total variances at the 0.02% level and below, so it seems unlikely that parameters $\psi_{\text{TrisH},M,\text{Cl}}$ would have an important effect.

The variance contributions in Fig. 11 are dominated by just three interactions at all salinities: those of $\text{TrisH}^+ - \text{HSO}_4^-$, those of $\text{TrisH}^+ - \text{Cl}^-$, and the ternary parameters $\theta_{\text{H},\text{TrisH}}$ and $\psi_{\text{H},\text{TrisH},\text{Cl}}$. The contribution of $\text{Na}^+ - \text{Cl}^-$, at no more than about 10% of the total variance, is the next most important. This result is a consequence of the fact that the change being made to the solutions is very simple: TrisH^+ is being substituted for Na^+ . The contribution of $\text{TrisH}^+ - \text{HSO}_4^-$ is particularly large because the parameters ($\beta^{(0,1)}_{\text{TrisH},\text{HSO}_4}$ and $C^{(0)}_{\text{TrisH},\text{HSO}_4}$) for this interaction are currently unknown, and this is reflected in the assigned uncertainties. The same is true for parameters $\theta_{\text{H},\text{TrisH}}$ and $\psi_{\text{H},\text{TrisH},\text{Cl}}$, which partly explains why their contributions to the total variances in Fig. 11 are much greater than those for $\theta_{\text{H},\text{Na}}$ and $\psi_{\text{H},\text{Na},\text{Cl}}$. Overall, we conclude that the dominance of just a few contributions the total calculated variance of ΔE^* makes it likely that the model will be relatively straightforward to improve for the calculation of this quantity.

6.4. Extrapolation of $\text{pH}_{\text{T},m}$ and $-\log_{10}(m\text{H}^+ + m\text{HSO}_4^-)$ to zero buffer molality

In the subsections above we have quantified the difference between $\text{pH}_{\text{T},m}$ and $\text{pH}^*_{\text{T},m}$ ($-\log_{10}(m\text{H}^+ + m\text{HSO}_4^-)$), expressing it in terms of ΔE^* and showing how it varies with the salinity of the buffer solution (Fig. 10). We have also discussed the meaning of an extrapolation of measured EMFs of a salinity 35 buffer solution to zero buffer molality (Fig. 6). This extrapolation is relevant to estimating the response of *m*-cresol indicator dye to pH in pure artificial seawater, unaffected by the presence of the buffer substance as would be the case in a real seawater measurement. In Fig. 12 we illustrate the relationship between $\text{pH}_{\text{T},m}$ and $\text{pH}^*_{\text{T},m}$, and their extrapolation to zero buffer molality in a salinity 35 artificial seawater. (All calculations in the figure used the revised $\text{TrisH}^+ - \text{Cl}^-$ parameters, $K(\text{HSO}_4^-)$ from Dickson et al. (1990), and unknown interaction parameters set to mean values taken from Appendix A in paper (I).) The dashed lines on the plots show $\text{pH}_{\text{T},m}$ as defined in Eq. (15), and the solid lines are $\text{pH}^*_{\text{T},m}$ which corresponds to the conventional thermodynamic total H^+ molality. For 0.04 mol kg^{-1} of buffer the two are calculated to differ by (0.0045 ± 0.0014) pH units. At buffer molalities less than about 0.02 mol kg^{-1} the buffering of pH is less effective, and both $\text{pH}_{\text{T},m}$ and $\text{pH}^*_{\text{T},m}$ tend towards a neutral pH for pure artificial seawater. DelValls and Dickson (1998) measured EMFs of these solutions to buffer molalities as low as 0.005 mol kg^{-1} , at which the decline in the calculated total pH, and of EMF, just exceeds the uncertainty in the measurements (the line ‘uncert. (ii)’ in Fig. 12a).

The fine dotted lines in Fig. 12a are fitted to a set of five points for each measure of pH. The pH of the intercept (point C), about 8.0738, can be understood as follows. First, taking the definition of $\text{pH}_{\text{T},m}$ (Eq. (15b)) and substituting Eq. (12) for E^* , and then Eq. (2) for $(E - E^0)$, yields:

$$\ln(m\text{H}^{+(\text{tr})}) = \ln(m\text{H}^+) + 2\ln(\gamma_{\text{HCl}}/\gamma_{\text{HCl}}^{(\text{tr})}) + \ln(1 + m\text{SO}_4^{2-(\text{tr})}/K^*(\text{HSO}_4^-)^{(\text{tr})}) \quad (17)$$

where $m\text{H}^+$ is the conventional thermodynamic molality of free H^+ , γ_{HCl} is the mean activity coefficient of HCl in the buffer solution, the superscript (tr) indicates quantities in pure artificial seawater of the same

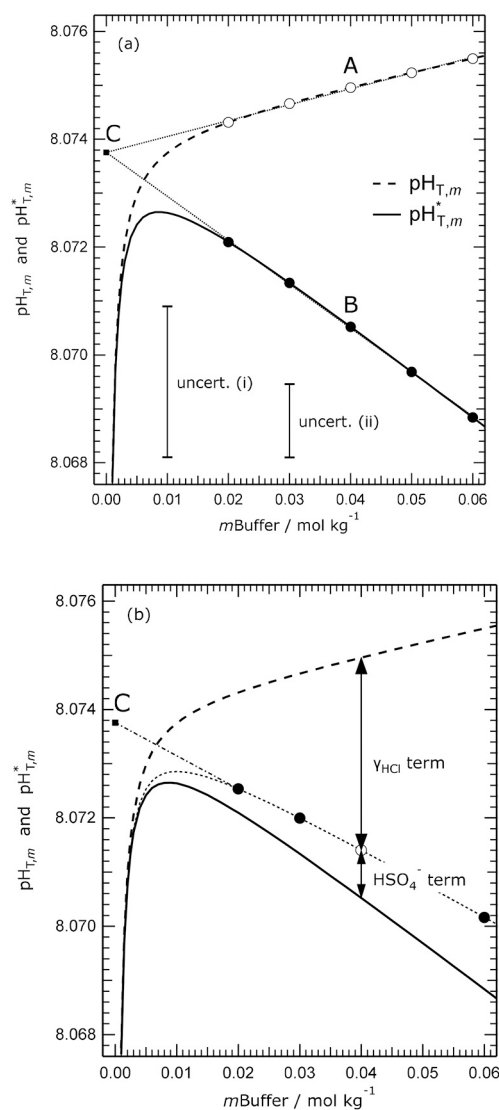


Fig. 12. Modelled values of total pH ($\text{pH}_{\text{T},m}$, defined in Eq. (15)) and $\text{pH}^*_{\text{T},m}$ ($-\log_{10}(m\text{H}^+ + m\text{HSO}_4^-)$), plotted against $\text{TrisH}^+/\text{Tris}$ buffer molality ($m\text{Buffer}$) for a salinity 35 artificial seawater at 25 °C. Symbols and lines on (a): circle, and dashed line – $\text{pH}_{\text{T},m}$; dot, and solid line – $\text{pH}^*_{\text{T},m}$. The fine dotted lines on plot (a) are extrapolations of linear fits to the two groups of points ($\text{pH}_{\text{T},m}$ and $\text{pH}^*_{\text{T},m}$) for buffer molalities of 0.02 to 0.06 mol kg^{-1} . The vertical distance between marked points A and B (about 0.0045 pH units) represents the influence of ΔE^* , see Eqs. (14) and (16b). The line ‘uncert. (i)’ on plot (a) indicates the effect of the uncertainty in ΔE^* (± 0.0014 molality-based pH units) on the difference between A and B, and ‘uncert. (ii)’ indicates the standard uncertainty of a typical EMF measurement (also in pH units). The two extrapolations (fine dotted lines) intercept at point C, for which $m\text{Buffer}$ is equal to zero. See the text for the meaning of this pH value. On plot (b) the meanings of the dashed and solid lines are the same as in (a), and the fine dotted line corresponds to the formal definition of total pH on a molal basis (Eq. (22)). The vertical distances between $\text{pH}^*_{\text{T},m}$ and $\text{pH}_{\text{T},m}$ and the fine dotted line indicate the magnitudes of the two terms that (added together) account for the differences between these quantities: ‘ HSO_4^- term’ is equal to $\ln[(1 + m\text{SO}_4^{2-(\text{tr})}/K^*(\text{HSO}_4^-)^{(\text{tr})})/(1 + m\text{SO}_4^{2-}/K^*(\text{HSO}_4^-))]$ (Eqs. (17) and (18)), and ‘ γ_{HCl} term’ is equal to $2\ln(\gamma_{\text{HCl}}/\gamma_{\text{HCl}}^{(\text{tr})})$ (Eq. (17)). The extrapolations of a linear fits of points on the fine dotted line (dots) intercepts the y-axis at $m\text{Buffer}$ equal to zero at the same point C as in plot (a).

salinity, and $m\text{SO}_4^{2-(\text{T})}$ is the total sulphate molality in an artificial seawater solution. The corresponding equation for the conventional thermodynamic total H^+ molality is:

$$\ln(m\text{H}^+ + m\text{HSO}_4^-) = \ln(m\text{H}^+) + \ln\left(1 + m\text{SO}_4^{2-}/K^*(\text{HSO}_4^-)\right) \quad (18)$$

where $m\text{H}^+$ has the same meaning as above, $m\text{SO}_4^{2-}$ is the molality of free sulphate in the buffer solution (effectively the same as the total sulphate in these alkaline solutions), and $K^*(\text{HSO}_4^-)$ is the stoichiometric dissociation constant of HSO_4^- in the buffer solution. It is clear that for a solution containing a trace molality of buffer, the value of $\gamma_{\text{HCl}}/\gamma_{\text{HCl}}^{(\text{tr})}$ in Eq. (17) must be unity, and the terms in sulphate molality in the two equations must be the same. Next, we take Eq. (18) above and replace $\ln(m\text{H}^+)$ by terms derived from the expression for the buffer equilibrium, so that:

$$\ln(m\text{H}^+ + m\text{HSO}_4^-) = \ln(K(\text{TrisH}^+)) + \ln(m\text{TrisH}^+/m\text{Tris}) + [2 \cdot \ln(\gamma_{\text{TrisHCl}}/(\gamma_{\text{HCl}} \cdot \gamma_{\text{Tris}}^{0.5})) + \ln(1 + m\text{SO}_4^{2-}/K^*(\text{HSO}_4^-))] \quad (19)$$

where $K(\text{TrisH}^+)$ is the thermodynamic equilibrium constant, and the quantities within the [] contain the activity coefficient terms that are a function of buffer molality. As was shown in Section 5.3, the molality quotient $m\text{TrisH}^+/m\text{Tris}$ is nearly constant above about 0.02 mol kg^{-1} of buffer, and the slopes of the lines for both $\text{pH}_{\text{T},m}$ and $\text{pH}^*_{\text{T},m}$ at higher buffer molalities are therefore the result of the changing activity coefficient terms alone. Consequently, point C on the plot is the value of $\text{pH}_{\text{T},m}$ or $\text{pH}^*_{\text{T},m}$ that a buffer solution (containing $>0.02 \text{ mol kg}^{-1}$ buffer) would have if all the relevant activity coefficients were equal to their trace values in pure artificial seawater. Put another way, all the components of artificial seawater have activity coefficient values that are unaltered by the buffer, and those of TrisH^+ and Tris are determined solely by interactions with the artificial seawater components and not with each other. Similarly, in Fig. 12b there is an additional curve plotted which corresponds to the formal total pH on a molal basis ($-\log_{10}((m\text{H}^+(\text{T}))_f)$, or $(\text{pH}_{\text{T},m})_f$), given by eq. (8) of DelValls and Dickson (1998). This curve also extrapolates linearly to point C in the same way as the other two measures in Fig. 12a. At this hypothetical but practically useful point, $\text{pH}_{\text{T},m}$, $(\text{pH}_{\text{T},m})_f$ and $\text{pH}^*_{\text{T},m}$ are identical.

What are the relative magnitudes of the terms that account for the differences between the three measures of pH? The difference between the operational and conventional thermodynamic total pH can be written as:

$$\begin{aligned} \text{pH}_{\text{T},m} - \text{pH}^*_{\text{T},m} &= -[\log_{10}(m\text{H}^+(\text{T})) - \log_{10}(m\text{H}^+ + m\text{HSO}_4^-)] \\ &= -2 \log_{10}(\gamma_{\text{HCl}}/\gamma_{\text{HCl}}^{(\text{tr})}) \\ &\quad - \log_{10}\left[\left(1 + m\text{SO}_4^{2-(\text{T})}/K^*(\text{HSO}_4^-)^{(\text{tr})}\right)/\left(1 + m\text{SO}_4^{2-}/K^*(\text{HSO}_4^-)\right)\right] \end{aligned} \quad (20)$$

The difference between the formal and conventional thermodynamic total pH involves only the $K^*(\text{HSO}_4^-)$ term:

$$\begin{aligned} (\text{pH}_{\text{T},m})_f - \text{pH}^*_{\text{T},m} &= -[\log_{10}((m\text{H}^+(\text{T}))_f) - \log_{10}(m\text{H}^+ + m\text{HSO}_4^-)] \\ &= -\log_{10}\left[\left(1 + m\text{SO}_4^{2-(\text{T})}/K^*(\text{HSO}_4^-)^{(\text{tr})}\right)/\left(1 + m\text{SO}_4^{2-}/K^*(\text{HSO}_4^-)\right)\right] \end{aligned} \quad (21)$$

The contributions of the HCl activity coefficient and $K^*(\text{HSO}_4^-)$ terms on the right-hand sides of the equations above are indicated in Fig. 12b. The term in the mean activity coefficient of HCl dominates, and accounts for most of the difference between the operational total pH ($\text{pH}_{\text{T},m}$, dashed line) and the conventional thermodynamic value ($\text{pH}^*_{\text{T},m}$, solid line). At a buffer molality of 0.04 mol kg^{-1} the value of the HCl activity coefficient term is about 0.0036 in pH, which is equivalent to the ratio $\gamma_{\text{HCl}}/\gamma_{\text{HCl}}^{(\text{tr})}$ of 0.9959. The fact that this ratio is so close to unity emphasises both the small size of these composition effects on activity

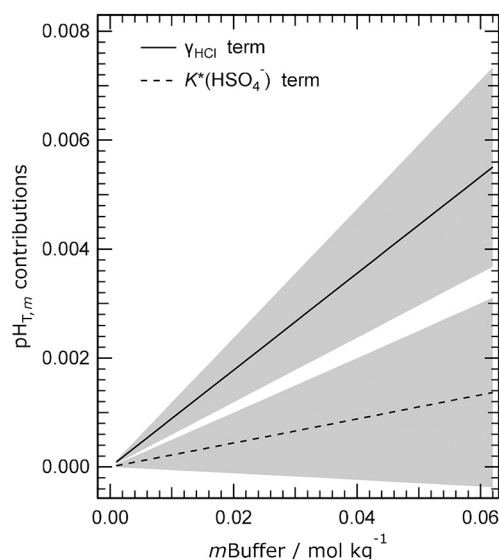


Fig. 13. Calculated values of the elements of ΔE^* (Eq. (14)) expressed as contributions to $\text{pH}_{\text{T},m}$, for a salinity 35 artificial seawater at 25°C containing various molalities of equimolar $\text{TrisH}^+/\text{Tris}$ buffer ($m\text{Buffer}$). Lines: solid – the term containing γ_{HCl} and $\gamma_{\text{HCl}}^{(\text{tr})}$; dash – the term containing $K^*(\text{HSO}_4^-)$ and $K^*(\text{HSO}_4^-)^{(\text{tr})}$. The calculated standard uncertainties are shown as shaded areas around each line.

coefficients in the buffer solutions, and the need for very great care in model development in order to quantify them accurately. The fine dotted line in Fig. 12b is equivalent to the formal total pH of the buffer ($(\text{pH}_{\text{T},m})_f$), which is discussed further in the next section. The estimated uncertainties in the HCl activity coefficient and $K^*(\text{HSO}_4^-)$ terms in eq. (20) are shown in Fig. 13. The uncertainty in the $K^*(\text{HSO}_4^-)$ term is very large relative to its value. The reason for this is apparent in Fig. 11d: the estimated variance contribution of the cation-anion interaction $\text{TrisH}^+ - \text{HSO}_4^-$ to ΔE^* is 50% of the total. This interaction does not contribute at all to $\gamma_{\text{HCl}}/\gamma_{\text{HCl}}^{(\text{tr})}$, and its effect is restricted to the $K^*(\text{HSO}_4^-)$ term in Eq. (20a) and to Eq. (14) for ΔE^* . The uncertainty is large because this interaction is unknown. Required improvements to the model are discussed in Section 7.

6.5. Linking total pH to the international system of units (SI)

It is apparent from Eqs. (20) and (21) that the operational total pH and hydrogen molality differ from the equivalent formal values as follows:

$$\begin{aligned} \text{pH}_{\text{T},m} - (\text{pH}_{\text{T},m})_f &= -[\log_{10}(m\text{H}^+(\text{T})) - \log_{10}((m\text{H}^+(\text{T}))_f)] \\ &= -2 \cdot \log_{10}(\gamma_{\text{HCl}}/\gamma_{\text{HCl}}^{(\text{tr})}) \end{aligned} \quad (22)$$

The activity coefficient term in Eq. (22) was explicitly neglected by DelValls and Dickson (1998) when assigning pH values of Tris buffers based upon Harned cell measurements and thereby calibrating operational pH (see our Eq. (15a)). The corresponding expression for formal total pH includes the term, so that:

$$(\text{pH}_{\text{T},m})_f = (F/\ln(10) \cdot RT)(E - E^*) + \log_{10}(m\text{Cl}^-) + 2 \cdot \log_{10}(\gamma_{\text{HCl}}/\gamma_{\text{HCl}}^{(\text{tr})}) \quad (23)$$

An ability to calculate the final term in Eq. (23) with well defined uncertainties should enable the formal total pH scale to be traceable to the SI: the uncertainties associated with measurements of E using Harned cells are quite well understood, and our results in paper (I) suggest that the empirical extrapolation by which E^* is obtained does not introduce any uncertainty over and above that in the measurements themselves. The uncertainty profiles shown in Fig. 11 for ΔE^* indicate

that the most important interaction parameters for the calculation of $\gamma_{\text{HCl}}/\gamma_{\text{HCl}}^{(\text{tr})}$ are those for $\text{H}^+\text{-TrisH}^+\text{-Cl}^-$ (which are unknown), TrisHCl , and to a lesser extent $\text{Na}^+\text{-Cl}^-$ and $\text{H}^+\text{-Na}^+\text{-Cl}^-$ (it is the differences between corresponding interactions that matter).

As noted in the previous section, the fine dotted line in Fig. 12(b) is equivalent to the $(\text{pH}_{\text{T},m})_f$ and is the sum of $\text{pH}_{\text{T},m}$ (the operational total pH) and the HCl activity coefficient term in Eq. (22). A linear extrapolation of $(\text{pH}_{\text{T},m})_f$ to a composition of pure artificial seawater (zero buffer molality) yields an intercept at the same value (8.0738, point C) as in Fig. 12a. As previously stated, in the limit of pure artificial seawater the three measures of total pH are therefore the same. This result can also be obtained directly from the equations above, and is consistent with the fact that the HCl activity coefficient and $K(\text{HSO}_4^-)$ terms, which are plotted in Fig. 13, are predicted to tend linearly to zero as buffer molality is reduced. It follows from this result that an experimentally determined estimate of this limiting value for $\text{pH}_{\text{T},m}$ can be used together with the Pitzer model described here and in paper (I) to obtain values of either of the other two measures of total pH for buffer solutions with finite amounts of Tris (these values cannot be determined experimentally).

7. Recommendations for future work

In section 8 of paper (I) we summarised the new measurements, and reassessments of existing data, that were needed to improve the current Pitzer-based speciation models of solutions containing the ions of acidified artificial seawater at temperatures from 0 °C to 45 °C, focusing particularly on representing the equilibrium between HSO_4^- and SO_4^{2-} . We also suggested general improvements needed for the estimation of uncertainties by the model (mainly the inclusion of Harned cell EMFs as a second representative data type). In this section we recommend

further work to increase the accuracy, and reduce the uncertainty, of the extension of the Waters and Millero (2013) model to include Tris buffers.

The uncertainty profiles in Figs. 2, 8, 9, and 11 identify the major contributors to the variances of model predictions of buffer EMF, the E^* difference term ΔE^* , and $\text{pH}_{\text{T},m}$ and $\text{pH}^*_{\text{T},m}$ at 25 °C. An improved representation of these interactions and equilibrium constants in the model should yield more accurate predictions for solutions containing the buffer species and the ions of artificial seawater. The effects of temperature are important: the strength of solute-solute interactions, and hence the magnitudes of the Pitzer interaction parameters, generally increase as temperature is reduced. These increases are likely to be large relative to the uncertainties in their values at 25 °C. It is therefore necessary to determine the variation with temperature of those interaction parameters that contribute more than a few percent to the total variance of the quantity being calculated. These contributors are listed in Table 9, together with the predicted quantities for which they are most important, and are briefly discussed below.

7.1. Aqueous TrisHCl

Interactions between TrisH^+ and Cl^- are the single most important ion interaction contribution to the calculated EMF of Tris buffer solutions (Fig. 2), and in the top three for the calculation of $\text{pH}^*_{\text{T},m}$, $\text{pH}^*_{\text{F},m}$ and ΔE^* (Figs. 8, 9, and 11). We have shown in Section 5.2 that the available measurements from which the cation-anion interaction parameters can be determined directly, at 25 °C, are likely to be subject to systematic errors. These are large enough to strongly influence calculated EMFs and pH on both scales. There is a clear need for new thermodynamic measurements from which the $\text{TrisH}^+\text{-Cl}^-$ parameters, and their variation with temperature, can be determined. These include EMFs, and also measurements of heats of dilution and heat capacities of

Table 9

Interactions and equilibrium constants that need reassessment.

Solutions or interactions	Parameters or equilibrium constants	T (existing)	E	ΔE^*	$\text{pH}^*_{\text{T},m}$	$\text{pH}^*_{\text{F},m}$	Notes
TrisHCl	$\beta^{(0,1)}_{\text{TrisH,Cl}}$, $C^{(0,1)}_{\text{TrisH,Cl}}$	25 °C	X	X	X	X	a
(TrisH)HSO ₄	$\beta^{(0,1)}_{\text{TrisH,HSO}_4}$, $C^{(0,1)}_{\text{TrisH,HSO}_4}$	–		X		x	b
$\text{H}^+\text{-TrisH}^+\text{-Cl}^-$	$\theta_{\text{H,TrisH}}$, $\psi_{\text{H,TrisH,Cl}}$	–		X		x	c
(TrisH) ₂ SO ₄	$\beta^{(0,1)}_{\text{TrisH,SO}_4}$, $C^{(0,1)}_{\text{TrisH,SO}_4}$	25 °C	x	X	x	x	d
Tris - Mg ²⁺	$\lambda_{\text{Tris,Mg}}$	25 °C	X		x	x	e
Tris - Na ⁺	$\lambda_{\text{Tris,Na}}$	25 °C	x		x	x	f
Other Interactions^g							
Tris buffer	$K(\text{TrisH}^+)$	f(T)	x				h
Tris-Ca ²⁺	$\lambda_{\text{Tris,Ca}}$	25 °C	x		x	x	i

Notes: This table lists the parameters and equilibrium constants that are the main contributors to the uncertainties of calculated EMFs (E), ΔE^* (Eq. (14)) and model-calculated $\text{pH}^*_{\text{T},m}$ and $\text{pH}^*_{\text{F},m}$ of Tris buffer in artificial seawater. The most significant are indicated by 'X', and those that contribute less by 'x'. The entry in the temperature column ('T') indicates whether the existing parameters or equilibrium constants are for the single temperature of 25 °C, or over a range of temperatures ('f(T)'). Parameters and equilibrium constants that are major contributors to calculated uncertainties in artificial seawater solutions only (i.e., they do not involve species TrisH^+ or Tris) are listed in table 5 of paper (I).

^a Values of the parameters for 25 °C have been determined by Lodeiro et al. (2021) and in the present work. Other data are that relevant are: EMFs of Bates and Hetzer (1961) (to 0.1 mol kg⁻¹ TrisHCl), EMFs of Tishchenko (2000) (mixtures with aqueous NaCl and Tris), EMFs of Macaskill and Bates (1975) (mixtures with aqueous HCl), equilibrium water vapour pressures (Lee and Lee, 1998), and apparent molar heat capacities of Ford et al. (2000) (to 0.5 mol kg⁻¹).

^b Values of these interaction parameters are not known.

^c These parameters can be determined at 25 °C from EMF measurements of $\text{H}^+\text{-TrisH}^+\text{-Cl}^-$ solutions by Macaskill and Bates (1975) and Bates and Macaskill (1985), but data for other temperatures are needed.

^d The only existing dataset for (TrisH)₂SO₄ is osmotic coefficients at 25 °C (Robinson and Bower, 1965). Values of these parameters, as functions of temperature, need to be known in order to obtain those for $\text{TrisH}^+\text{-HSO}_4^-$ interactions from data for acidified (TrisH)₂SO₄ solutions.

^e Calculations using an uncertainty for this parameter from the fits in Section 2 yielded enhanced variance contributions to the calculated E, $\text{pH}^*_{\text{T},m}$, and $\text{pH}^*_{\text{F},m}$ relative to the base case. The variation with temperature of this strong interaction is unknown.

^f Values of this parameter at different temperatures can be determined from solubility measurements of Lodeiro et al. (2021). However, comparisons made at 25 °C by Lodeiro et al. suggest some inconsistencies between datasets. This parameter should be redetermined.

^g Other interactions, for which the differential of the buffer EMF with respect to the parameter is generally at a level of 10–20% of more of the highest value.

^h The standard uncertainty in $K(\text{TrisH}^+)$ makes only a small (5%) contribution to the calculated variance, but may be worth reassessing as a part of the determination of the $\text{TrisH}^+\text{-Cl}^-$ parameters from EMF data.

ⁱ This strong interaction has only a small influence on the calculated E, $\text{pH}^*_{\text{T},m}$, and $\text{pH}^*_{\text{F},m}$ because of its low concentration in seawater relative to other ions. However, this may not be true of other natural waters (and buffer solutions of corresponding composition). Also, it is only known from a single dataset at 25 °C.

aqueous TrisHCl from which the variation with temperature of the interaction parameters can be determined.

7.2. TrisH^+ - HSO_4^- and TrisH^+ - SO_4^{2-} interactions

The parameters for TrisH^+ - HSO_4^- are found to be very important for the calculation of ΔE^* . Although the values of these parameters are currently unknown, they could in principle be determined from EMFs of Harned cells containing aqueous $(\text{TrisH})_2\text{SO}_4$ and HCl. This requires that the parameters for TrisH^+ - SO_4^{2-} and TrisH^+ - Cl^- interactions are also known. Those for TrisH^+ - SO_4^{2-} also contribute a few percent to the variance of the calculated EMF of Tris buffer (Fig. 2). It is possible that this is an underestimate, if the single set of osmotic coefficient measurements which the parameters were determined from are subject to systematic error as appears to have been the case for similar data for aqueous TrisHCl (Section 5.2). Interaction parameters for TrisH^+ - SO_4^{2-} interactions can also be determined from EMF measurements yielding the activity product $a\text{H}^+ \cdot a\text{Cl}^-$ although the presence of Cl^- ions means that ternary parameters (e.g., $\theta_{\text{Cl},\text{SO}_4}$ and $\psi_{\text{Cl},\text{SO}_4,\text{TrisH}}$) could also have a large influence. The same types of thermal measurements, of aqueous $(\text{TrisH})_2\text{SO}_4$ solutions, as noted above for aqueous TrisHCl, would be valuable.

7.3. H^+ - TrisH^+ - Cl^- interactions

The parameters $\theta_{\text{H},\text{TrisH}}$ and $\psi_{\text{H},\text{TrisH},\text{Cl}}$ are major contributors to the variance of calculated ΔE^* , and their values at 25 °C can be determined from available EMF measurements (Macaskill and Bates, 1975). Their variation with temperature can be determined from similar measurements at other temperatures, together with a knowledge of the values of TrisH^+ - Cl^- and H^+ - Cl^- interaction parameters.

7.4. Tris-cation interactions

The uncertainty contributions of parameters $\lambda_{\text{Tris},\text{Na}}$ and $\lambda_{\text{Tris},\text{Mg}}$ are a few percent for the calculation of buffer EMF, $\text{pH}_{\text{T},m}$ and $\text{pH}^*_{\text{T},m}$ (see Fig. 9, and the discussion in Section 5.2). However, their variation with temperature is unknown, and the Tris- Mg^{2+} interaction is particularly strong. The same is true of Tris- Ca^{2+} , although it has a much lower molality in artificial seawater than Mg^{2+} . The values of the interaction parameters at 25 °C have been determined either from a single dataset, or (in the case of $\lambda_{\text{Tris},\text{Na}}$) there appear to be inconsistencies between different sets of measurements (Lodeiro et al., 2021), or the parameters are only determinable as pairs such as $(\theta_{\text{TrisH},\text{M}} - \lambda_{\text{Tris},\text{M}})$ which is the case for the potentiometric titration measurements discussed in Section 2. Other types of data that would be valuable for determining these interaction parameters over the full temperature range include further solubility measurements similar to those of Lodeiro et al. (2021), and also EMFs of Tris buffer in various simple metal chloride solutions (although these involve co-determination of $\lambda_{\text{Tris},\text{M}}$ with other interaction parameters).

7.5. Other interactions

We have listed the dissociation constant $K(\text{TrisH}^+)$ in Table 9 chiefly because its determination from EMF measurements of dilute equimolar TrisHCl and Tris can also yield values of γ_{TrisHCl} , as described in Section 5.2. A redetermination of $K(\text{TrisH}^+)$, using modern values of the Debye-Hückel constant and the activity coefficient expression that includes it, and a calculation of the equilibrium between TrisH^+ and Tris (rather than assuming that they retain their stoichiometric values as was done in the analysis of Bates and Hetzer (1961)), may yield improved values of both $K(\text{TrisH}^+)$ and γ_{TrisHCl} . The results of Ford et al. (2000) for the heat

capacity change of the dissociation reaction are likely to be an important constraint.

The parameter $\lambda_{\text{Tris},\text{Ca}}$ is listed in the table for similar reasons as $\lambda_{\text{Tris},\text{Mg}}$, and may be an important contributor in waters with a higher Ca^{2+} concentration than seawater.

8. Summary and discussion

In this work we have extended the speciation model described in paper (I) to include Tris buffer species at 25 °C. We have used the model to investigate some of the technical aspects of the total pH scale, and its inherent assumptions, that are relevant to its extension to low salinities and to linking model calculations of acid-base equilibria in seawater to measured pH_{T} . The main example of this is the ΔE^* term which represents assumptions inherent in the calibration of the total pH scale using Harned cell measurements. Our principal results are as follows:

First, in Section 5.2 (and following on in Section 7) we have identified aqueous solutions for which new thermodynamic activity measurements should be made to improve and complete the model (Table 9), additional to what was proposed in paper (I). For these buffer solutions the measurements are relatively few: essentially aqueous TrisHCl and $\text{TrisH}_2\text{SO}_4$, acidified sulphate solutions that allow interactions between TrisH^+ and HSO_4^- ions to be quantified, and mixtures containing dissolved Tris and chloride salts of major seawater cations. Interaction parameter values can be obtained from any thermodynamic measurement that yields activities: for example EMFs, potentiometric titrations, isopiestic or vapour pressure measurements yielding osmotic coefficients, or thermal measurements (heats of dilution or heat capacities) from which first and second partial derivatives of the interaction parameters with respect to temperature can be obtained.

Second, in Section 5.3 we showed that the change in buffer solution EMF (hence $\text{pH}_{\text{T},m}$) with buffer molality can be divided into two elements: an activity coefficient term which is linear with respect to the molality of the buffer in a particular artificial seawater at all buffer molalities, and a smaller term in the equilibrium $m\text{TrisH}^+/m\text{Tris}$ ratio which only becomes significant below about 0.01 to 0.02 mol kg^{-1} of buffer. This is valuable for understanding the procedure of extrapolating measured buffer EMF to a composition of pure artificial seawater, and its limitations. An ability to calculate the activity coefficient term directly will be particularly valuable for extending the total pH scale to very low salinities for which the range of possible buffer molalities (where TrisH^+ is substituted for Na^+) is necessarily small. The results also suggest, together with those for the ΔE^* term, that a buffer molality of 0.02 mol kg^{-1} may be appropriate for establishing pH scales for salinities as low as 2.

Third, it was demonstrated in Section 5.4 that the change in buffer EMF and consequently $\text{pH}_{\text{T},m}$ with $\text{TrisH}^+:\text{Tris}$ ratio can be calculated satisfactorily according to a very simple relationship (Eq. (8)). This does not require the use of the model, and should be useful for the preparation of buffers with a higher or lower pH_{T} than normal.

Fourth, in Section 6.3 we have quantified, for the first time, the ΔE^* term that links the operationally defined total H^+ ion molality obtained from the $\text{pH}_{\text{T},m}$ of Tris buffers with the conventional thermodynamic total ($m\text{H}^+ + m\text{HSO}_4^-$) in the solution. Calculations show that the value of ΔE^* increases as salinity is reduced, as expected, but only by about 50% relative to its value in the 20 to 40 salinity range. This implies that the total pH scale can be straightforwardly extended to much lower salinities – perhaps as low as 5, or even 2 if buffer molalities are reduced – using the approach of DelValls and Dickson (1998). Their substitution of TrisH^+ for Na^+ in the buffer solutions, with no other changes of composition, also makes ΔE^* more likely to be modelled accurately than other approaches (such as that of Müller et al., 2018) because the uncertainty contributions are then dominated by only a few parameters.

Furthermore the ability to calculate, in addition to ΔE^* , free H^+ (mH^+) and HSO_4^- ($mHSO_4^-$) in seawater permits the conversion of stoichiometric equilibrium constants (e.g. K_1 and K_2 of the dissolved CO_2 system) determined on the total pH scale to a free H^+ basis that would be consistent with the treatment of many other acid-base and complexation equilibria.

Fifth, we have examined in Section 6.4 the difference between $pH_{T,m}$ and $-\log_{10}(mH^+ + mHSO_4^-)$ (i.e., $pH^*_{T,m}$), which is equivalent to ΔE^* above, and have calculated the contributions of the two terms that account of the difference (one in γ_{HCl} , and one in $K^*(HSO_4^-)$, see Eq. (20)). We have established the meaning of the linear extrapolation of $pH_{T,m}$ to zero buffer molality (analogous to the extrapolation of EMF in Section

Chart 1

Relationships between different measures of pH.

For simplicity, the relationships below are expressed in terms of molalities. To convert each measure of pH to a moles per kg of seawater basis, use Eq. (A.5) in the Appendix. For example, $pH_T = pH_{T,m} - \log_{10}(1 - 0.00100198 \cdot S)$, where S is the nominal salinity of an artificial seawater sample.

1. $pH^*_{F,m}$ ($= -\log_{10}(mH^+)$)

The quantity mH^+ is the conventional thermodynamic free H^+ molality in a solution. It is calculated directly (although with some uncertainty) by chemical speciation models of acid–base equilibria, but cannot be measured directly in seawater.

2. $pH^*_{T,m}$ ($= -\log_{10}(mH^+ + mHSO_4^-)$)

The sum ($mH^+ + mHSO_4^-$) is the conventional thermodynamic total H^+ molality in a solution, and is calculated directly (although with some uncertainty) by chemical speciation models. It cannot be measured directly in seawater. The quantities $pH^*_{F,m}$ and $pH^*_{T,m}$ are related by:

$$pH^*_{T,m} = pH^*_{F,m} - \log_{10}(1 + mSO_4^{2-}/K^*(HSO_4^-))$$

where mSO_4^{2-} is the free SO_4^{2-} molality, and $K^*(HSO_4^-)$ the stoichiometric dissociation constant of HSO_4^- in the solution of interest. For seawater solutions of $pH > 5$, mSO_4^{2-} is effectively the total SO_4^{2-} molality – because $mHSO_4^-$ is much less than mSO_4^{2-} – and consequently $K^*(HSO_4^-)$ is invariant with pH. In these solutions, the difference between $pH^*_{T,m}$ and $pH^*_{F,m}$ is therefore constant at a given solution composition (salinity), temperature, and pressure.

3. $pH_{T,m}$

The quantity $pH_{T,m}$ is the operationally defined total pH (on a molality basis) of DelValls and Dickson (1998), see their eqs. (8) and (9). In this work the relationship between $pH_{T,m}$ and the EMFs of the Tris buffer solutions used to calibrate the total pH scale is given by Eq. (15b). The relationship between $pH_{T,m}$ and $pH^*_{T,m}$ in Tris buffer solutions is, from our Eq. (16):

$$pH_{T,m} = pH^*_{T,m} + (F/[\ln(10) \cdot RT]) \cdot \Delta E^*$$

where ΔE^* is given by Eq. (14). The quantity ΔE^* cannot be determined experimentally, but it can be estimated using models.

4. $pH_{F,m}$

The quantity $pH_{F,m}$ is the free pH (i.e., the measure of H^+ molality *not* including HSO_4^-) that is implicit in the definition of the operational total pH above. The relationship between $pH_{F,m}$ and $pH_{T,m}$ is similar to that between $-\log_{10}(mH^+)$ and $-\log_{10}(mH^+ + mHSO_4^-)$:

$$pH_{F,m} = pH_{T,m} + \log_{10}(1 + mSO_4^{2-(T)}/K^*(HSO_4^-)^{(tr)})$$

The difference between $pH_{F,m}$ and $pH_{T,m}$ (at constant salinity, temperature, and pressure) is fixed, according to this definition. For neutral and basic conditions this is an excellent approximation. Using the definition from item (3) above, and the restriction that the relationship applies to neutral and basic solutions, the measure of conventional thermodynamic free H^+ molality, $pH^*_{F,m}$, is related to the $pH_{T,m}$ of a seawater sample by:

$$pH^*_{F,m} \approx (pH_{T,m} - (F/[\ln(10) \cdot RT]) \cdot \Delta E^*) + \log_{10}(1 + mSO_4^{2-(T)}/K^*(HSO_4^-)^{(tr)})$$

5. $(pH_{T,m})_f$

The quantity $(pH_{T,m})_f$, equal to $-\log_{10}((mH^{+(T)})_f)$, is the formal total pH on a molality basis, where:

$$(mH^{+(T)})_f = mH^+(1 + mSO_4^{2-(T)}/K^*(HSO_4^-)^{(tr)})$$

This formal total hydrogen ion molality $(mH^{+(T)})_f$ was defined by Dickson (1990), see his eq. (10). It is also given by DelValls and Dickson (1998) in their eq. (8). In this work the relationship between $(pH_{T,m})_f$ and the Harned cell EMFs of the Tris buffer solutions used to calibrate the total pH scale is given by Eq. (23). The formal total pH will have the same numerical values as the operational total pH ($pH_{T,m}$) in artificial seawater, or seawater, but differs in other solutions such as Tris buffers because γ_{HCl} will not be equal to $\gamma_{HCl}^{(tr)}$ (see the final term in eq. (7) of DelValls and Dickson (1998)).

5.3) and shown that at this limit $\text{pH}_{T,m}$, $-\log_{10}(m\text{H}^+ + m\text{HSO}_4^-)$, and the formal total pH ($\text{pH}_{T,m,f}$) are the same. The different measures of total pH, and their relationships with conventional thermodynamic total and free H^+ molalities, are summarised in [Chart 1](#).

The ability to calculate the influence of the difference term ΔE^* (Eq. (14)) is important for the comparisons of $\text{pH}_{T,m}$ with conventional thermodynamic values of $m\text{H}^+$ and $(m\text{H}^+ + m\text{HSO}_4^-)$, as noted above. We have shown that it is possible to obtain agreement between a measurement-based and calculated $\text{pH}_{T,m}$ to within 0.002 pH units, and between a measurement-based and calculated $-\log_{10}(m\text{H}^+ + m\text{HSO}_4^-)$ to within 0.003 pH units, all at 25 °C (see [Table 8](#)). This level of accuracy suggests that a more fully developed model will be able to meet the needs of marine chemists.

The magnitude of the difference between $\text{pH}_{T,m}$ and $-\log_{10}(m\text{H}^+ + m\text{HSO}_4^-)$, which is shown in [Fig. 12](#) for an equimolar Tris buffer in a salinity 35 seawater at 25 °C, may have practical consequences. Stoichiometric equilibrium constants for carbonate equilibria in seawater (e.g., [Millero et al. \(2006\)](#) and references therein) are defined in terms of total hydrogen ion concentration, and are intended for use with measurements of seawater pH on the total scale. Whether the hydrogen ion concentration terms in these constants, when expressed on the molality scale, correspond more closely to $m\text{H}^{+(\text{T})}$ (from $\text{pH}_{T,m}$), $m\text{H}^{+(\text{T})}_f$, or to the conventional thermodynamic total $(m\text{H}^+ + m\text{HSO}_4^-)$ depends upon the details of the experimental method used to determine their values. Our results in [Fig. 12](#) show that the difference between $m\text{H}^{+(\text{T})}$ and $(m\text{H}^+ + m\text{HSO}_4^-)$ in Tris buffer solutions is as much as 0.0045 in pH. Further investigation into how total pH is implicitly defined in the measured values of the carbonate constants in seawater media is needed.

The linking of the formal total pH scale to SI base units requires a quantification of uncertainties at each stage from fundamental measurements (of the EMFs of Tris buffers, and of acidified artificial seawater) to defined $(\text{pH}_{T,m})_f$, including any simplifying assumptions made. The use of the model to estimate the activity coefficient quotient $\gamma_{\text{HCl}}/\gamma_{\text{HCl}}^{(\text{tr})}$ is the first quantification of this neglected term that is inherent in the definition of $(\text{pH}_{T,m})_f$, and therefore a step towards establishing the link with the SI. In order to complete this, further work needs to be done to improve the models for the key interactions noted in [Section 6.5](#), and particularly to establish the uncertainties associated with the relevant Pitzer interaction parameters (rather than simulate them on the basis of assumed datasets, which is done throughout this work as described in detail in paper (I)).

We have not addressed the definition of a free pH scale ($\text{pH}_{F,m}$) based upon EMF measurements of Tris buffer solutions in artificial seawater (see, for example, [Waters and Millero, 2013](#)), although we have determined the uncertainty profile for the calculation of $-\log_{10}(m\text{H}^+)$ ($\text{pH}^*_{F,m}$) in Tris buffer solutions. It would be possible to establish such a scale, entirely independent of $K^*(\text{HSO}_4^-)$, in two ways. First, from the accurate calculation of γ_{HCl} in the Tris buffer solutions using the model, in which case an independently determined E^* would not be required and $\text{pH}_{F,m}$ would be equal to $-\log_{10}(m\text{H}^+)$ (i.e., $\text{pH}^*_{F,m}$, as there would be no ΔE^* term). Second, it could be done if values of E^* were obtained in the same way as by [Dickson \(1990\)](#), but for artificial seawater not containing SO_4^{2-} . In this case the ΔE^* term might be larger than for the definition of $\text{pH}_{T,m}$, and model would still be required to convert from $\text{pH}_{F,m}$ to the conventional thermodynamic $-\log_{10}(m\text{H}^+)$. The work of [Camões et al. \(2016\)](#) is relevant to this point. A pH_F scale extending to salinity 5, or the ability to calculate $m\text{H}^+$ from $\text{pH}_{T,m}$ to a quantified uncertainty to the same low salinity, would be a significant step towards linking to the IUPAC pH scale ($\text{pH} = -\log_{10}(a\text{H}^+)$) ([Buck et al., 2002](#))

and integration with freshwater pH measurements.

We have also not investigated the calculation of $a\text{H}^+ \cdot a\text{Cl}^-$ activity products, or the quotient $a\text{H}^+/a\text{Na}^+$ for use in the calibration of H^+/Cl^- and H^+/Na^+ electrode pairs for the measurement of pH. However, it is apparent that the uncertainty profile for $a\text{H}^+ \cdot a\text{Cl}^-$ will be the same as for the EMF of the Harned cell, and for $a\text{H}^+/a\text{Na}^+$ it is likely that interactions $\text{H}^+ \cdot \text{Cl}^-$, $\text{Na}^+ \cdot \text{Cl}^-$, and $\text{H}^+ \cdot \text{Na}^+ \cdot \text{Cl}^-$ (and H^+ and Na^+ with SO_4^{2-}) will dominate simply on the basis of artificial seawater composition.

The results described in this work have been obtained at 25 °C only, using the model with TrisH^+ and Tris interaction parameters some of which are preliminary values. Nonetheless these results give confidence that the practical aims outlined in the Introduction can be achieved with a model of solutions containing the ions present in acidified artificial seawater (paper (I)), and extended to include Tris buffer in artificial seawater (this work). Further development is needed to: (i) extend the model to 0 to 45 °C for interactions involving the buffer species; (ii) revise some interaction parameters and equilibrium constants to improve model accuracy; and (iii) extend the treatment of uncertainties to, for example, include EMFs as a second fundamental data type. An important addition to item (iii) would be to treat explicitly the uncertainties associated with the major contributors identified in the uncertainty profiles (e.g., $\text{TrisH}^+ \cdot \text{Cl}^-$ interactions) rather than apply the simulation methods described in paper (I) and in the Supporting Information to this work.

What are the implications for the use and future development of the total pH scale? Our results suggest that attention should be given to understanding the consistency of the experimentally determined K^* for acid-base equilibria in seawater media. These typically include a measure of total pH in their formulation. In future, the ability to calculate the influence of the ions of seawater on TrisH^+ and Tris activities in buffer solutions should enable the total pH scale to be extended to lower salinities, and the total H^+ concentration of buffers in solutions of non-seawater stoichiometry to be defined. Both these things are likely to be of practical use. More broadly, an accurate and self-consistent model of acid-base equilibria and speciation in solutions containing the ions of seawater will have applications in diverse fields such ocean acidification, the study of past ocean environments, and mineral formation.

Declaration of Competing Interest

None.

Acknowledgements

The work of S.L.C. and M.P.H. was supported by the Natural Environment Research Council of the UK (award NE/P012361/1), and A.G.D. by the U.S. National Science Foundation (award OCE-1744653), both under the joint NERC/NSF:GEO scheme. The contribution of J.F.W. was supported by the National Institute of Standards and Technology of the U.S.A. This publication is a contribution of SCOR Working Group 145 (SCOR is the Scientific Committee on Oceanic Research) and of the Joint Committee on Seawater which is sponsored by SCOR, the International Association for the Properties of Water and Steam, and the International Association for the Physical Sciences of the Oceans. The work of WG 145 presented in this article results, in part, from funding provided by national committees of SCOR and from a grant to SCOR from the U.S. National Science Foundation (OCE-1840868).

Appendix A

1. Quantities for expressing the composition of seawater solutions

This work, and paper (I), use molalities for solute species (moles per kg of pure water solvent) exclusively, while oceanographers often use amount content (moles per kg of seawater). The two are related, for any solute species i , by:

$$C(i) = m(i) / [1 + \sum_i m(i) \cdot M_w(i)] \quad (\text{A.1})$$

where $C(i)$ is the amount content of species i in moles per kg of solution, $m(i)$ is the molality of species i , and $M_w(i)$ is the molar mass of species i in kg. For cases where the solute amount contents are known, the following equation can be used for conversion:

$$m(i) = C(i) / [1 - \sum_i C(i) \cdot M_w(i)] \quad (\text{A.2})$$

For an artificial seawater of the composition given by [Dickson \(1990\)](#), and with a known nominal salinity S , the conversion is given by:

$$C(i) = m(i) \cdot [1 - 0.00100198 \cdot S] \quad (\text{A.3})$$

The numerical factor in the above equation is equal to 0.0350693/35, where 0.0350693 kg is the total mass of the five salts present in 1 kg of this artificial seawater of nominal salinity 35. For a seawater of the Reference Composition (see table 4 of [Millero et al. \(2008\)](#)), with a known Practical Salinity S_p , the equivalent equation is:

$$C(i) = m(i) \cdot [1 - 0.001004715 \cdot S_p] \quad (\text{A.4})$$

In this case the numerical factor is equal to 0.03516504/35, where 0.03516504 kg is the defined solute content of seawater of the Reference Composition corresponding to a Practical Salinity of exactly 35 (and based upon atomic weights of 2005 which are listed in Table 12 of [Millero et al. \(2008\)](#)). Eq. (A.3) can be applied to convert any of the pH measures described in this work between the molality and amount content of seawater scales, for example:

$$\text{pH} = \text{pH}_m - \log_{10}(1 - 0.00100198 \cdot S) \quad (\text{A.5})$$

where pH_m is the molality-based pH in the artificial seawater.

For a natural seawater, a similar conversion can be achieved based on Eq. (A.4):

$$\text{pH} = \text{pH}_m - \log_{10}(1 - 0.001004715 \cdot S_p) \quad (\text{A.6})$$

2. Definitions of pH, and terminology

Solutions of artificial seawater containing Tris buffer contain the major solute species Na^+ , Mg^{2+} , Ca^{2+} , K^+ , TrisH^+ , Cl^- , SO_4^{2-} and Tris. For the purposes of calculating acid-base equilibria H^+ , HSO_4^- , OH^- , and the ion pair MgOH^+ are added. There are four equilibria: the dissociations of solutes TrisH^+ , HSO_4^- , and MgOH^+ , and equilibrium between the solvent H_2O and H^+ and OH^- . The activities and concentrations of these species, in aqueous solutions of all compositions comprising the above solutes, are described using standard thermodynamic relationships for equilibrium constants and solute and solvent activities (e.g., [Pitzer, 1995](#)). Species molalities that conform to the above relationships are referred to in this work as *conventional thermodynamic molalities*.

For Tris buffer solutions the procedure for establishing an operationally defined total pH ($\text{pH}_{T,m}$), which is an estimate of the sum of H^+ and HSO_4^- molalities, involves assumptions concerning the mean activity coefficient of HCl and the value of $K^*(\text{HSO}_4^-)$ (the stoichiometric dissociation constant or molality quotient $m\text{H}^+ \cdot m\text{SO}_4^{2-} / m\text{HSO}_4^-$, see [Section 6](#)). We refer to the total H^+ molality obtained from $\text{pH}_{T,m}$ as the *operationally defined total H^+ molality*, or $m\text{H}^{+(\text{T})}$, to distinguish it from the conventional thermodynamic total molality ($m\text{H}^+ + m\text{HSO}_4^-$).

The formal total pH ($\text{pH}_{T,m,f}$), like total pH above, is a measure of the sum of H^+ and HSO_4^- molalities but differs from $\text{pH}_{T,m}$ in that the definition does not make any assumptions concerning the mean activity coefficient of HCl in the solution of interest. We refer to the total H^+ molality obtained from ($\text{pH}_{T,m,f}$) as the *formal total H^+ molality*, or $(m\text{H}^{+(\text{T})})_f$.

In the equations for total pH presented in [Section 6](#) we refer to trace values (e.g., the mean activity coefficient of HCl, and stoichiometric dissociation constant of HSO_4^-), indicated by the superscript (tr). This refers to the value of the quantity of interest in the limit of the pure background medium (here an artificial seawater). Its determination from measurement involves extrapolation of the quantity, for a series of added HCl molalities, to the composition of pure artificial seawater (and added $m\text{HCl}$ equal to zero). Using the Pitzer or other speciation model the values of the trace quantity of interest, on a conventional thermodynamic basis, can be calculated directly for the medium composition corresponding to the limiting case.

The relationships between the different measures of pH used in this work are summarised in [Chart 1](#).

Appendix B. Supplementary data

There are seven numbered documents of supporting information. The first document summarises the contents of the others, and lists the tables and charts that appear in each one. The subjects covered are: the simulation of uncertainties; values of variances and covariances for interactions and equilibrium constants involving TrisH^+ and Tris; values of the Pitzer parameters and equilibrium constants; and calculated equilibrium solute molalities and activity coefficients for program verification. The model described in this work is an extension of the 'base' model for artificial seawater described in paper (I), which should be consulted for details of the treatment of the ions of artificial seawater. It is anticipated that software tools incorporating the models will be released in late 2022 (see website marchemspec.org for future announcements, or contact the corresponding author). Supplementary data to this article can be found online at <https://doi.org/10.1016/j.marchem.2022.104096>.

References

- Archer, D.G., 1992. Thermodynamic properties of the NaCl + H₂O system II. Thermodynamic properties of NaCl(aq), NaCl.2H₂O(cr), and phase equilibria. *J. Phys. Chem. Ref. Data* 21, 793–829.
- Bates, R.G., Hetzer, H.B., 1961. Dissociation constant of the protonated acid form of 2-amino-2-(hydroxymethyl)-1,3-propanediol [tris-(hydroxymethyl)-aminomethane] and related thermodynamic quantities from 0 to 50°. *J. Phys. Chem.* 65, 667–671.
- Bates, R.G., Macaskill, J.B., 1985. Activity and osmotic coefficients of t-butylammonium chloride: activity of HCl in mixtures with TRIS hydrochloride and t-butylammonium chloride at 25 °C. *J. Soln. Chem.* 14, 723–734.
- Bates, R.G., Pinching, G.D., 1949. Dissociation constants of weak bases from electromotive-force measurements of solutions of partially hydrolyzed salts. *J. Res. Natl. Bur. Stand.* 43, 519–526.
- Buck, R.P., Rondinini, S., Covington, A.K., Baucke, F.G.K., Brett, C.M.A., Camões, M.F., Milton, M.J.T., Mussini, T., Naumann, R., Pratt, K.W., Spitzer, P., Wilson, G.S., 2002. Measurement of pH. Definition, standards, and procedures. *Pure Appl. Chem.* 74 (11), 2169–2200.
- Camões, M.F., Anes, B., Martins, H., Oliveira, C., Físicaro, P., Stoica, D., Spitzer, P., 2016. Assessment of H⁺ in complex aqueous solutions approaching seawater. *J. Electroanal. Chem.* 764, 88–92.
- Campbell, D.M., Millero, F.J., Roy, R.N., Roy, L.N., Lawson, M., Vogel, K.M., Porter-Moore, C., 1993. The standard potential for the hydrogen-silver, silver chloride electrode in synthetic seawater. *Mar. Chem.* 44, 221–233.
- Clegg, S.L., Whitfield, M., 1995. A chemical model of seawater including dissolved ammonia, and the stoichiometric dissociation constant of ammonia in estuarine water and seawater from –2° to 40 °C. *Geochim. Cosmochim. Acta* 59, 2403–2421.
- Clegg, S.L., Rard, J.A., Pitzer, K.S., 1994. Thermodynamic properties of 0.6 mol kg⁻¹ aqueous sulphuric acid from 273.15 to 328.15 K. *J. Chem. Soc. Faraday Trans.* 90, 1875–1894.
- DelValls, T.A., Dickson, A.G., 1998. The pH of buffers based on 2-amino-2-(hydroxymethyl)-1,3-propanediol (“tris”) in synthetic sea water. *Deep-Sea Res.* 1 45, 1541–1554.
- Dickson, A.G., 1990. Standard potential of the (Ag(s) + 1/2H₂(g) = Ag(s) + HCl(aq)) cell and the dissociation constant of bisulphate ion in synthetic seawater from 273.15 to 318.15K. *J. Chem. Thermodynamics* 22, 113–127.
- Dickson, A.G., Wesolowski, D.J., Palmer, D.A., Mesmer, R.E., 1990. Dissociation constant of bisulphate ion in aqueous sodium chloride solutions to 250 °C. *J. Phys. Chem.* 94, 7978–7985.
- Dickson, A.G., Sabine, C.L., Christian, J.R. (Eds.), 2007. Guide to Best Practices for Ocean CO₂ Measurements. North Pacific Marine Science Organisation. PICES Special Publication 3; IOCCP Report No. 8. 176pp.
- Dickson, A.G., Camões, M.F., Spitzer, P., Físicaro, P., Stoica, D., Pawlowicz, R., Feistel, R., 2016. Metrological challenges for measurements of key climatological observables. Part 3: seawater. *Metrologia* 53, R26–R39.
- Ford, T.D., Call, T.G., Origlia, M.L., Stark, M.A., Woolley, E.M., 2000. Apparent molar volumes and apparent molar heat capacities of aqueous 2-amino-2-(hydroxymethyl)-propan-1,3-diol (Tris or THAM) and THAM plus equimolar HCl. *J. Chem. Thermodyn.* 32, 499–516.
- Glasstone, S., Schram, A.F., 1947. The basic dissociation constants of some aliphatic hydroxyamines. *J. Amer. Chem. Soc.* 69, 1213–1214.
- Humphreys, M.P., Waters, J.F., Turner, D.R., Dickson, A.G., Clegg, S.L., 2022. Chemical speciation models based upon the Pitzer activity coefficient equations, including the propagation of uncertainties: artificial seawater from 0 to 45 °C. *Mar. Chem.* <https://doi.org/10.1016/j.marchem.2022.104095>.
- Kho, K.H., Ramette, R.W., Culberson, C.H., Bates, R.G., 1977. Determination of hydrogen ion concentrations in seawater from 5 to 40 °C: standard potentials at salinities from 20 to 45 ppt. *Anal. Chem.* 49, 29–34.
- Lee, L., Lee, C., 1998. Vapor pressures and enthalpies of vaporization of aqueous solutions of triethylammonium chloride, 2-hydroxyethylammonium chloride, and tris(hydroxymethyl)aminomethane hydrochloride. *J. Chem. Eng. Data* 43, 469–472.
- Lodeiro, P., Turner, D.R., Achterberg, E.P., Gregson, F.K.A., Reid, J.P., Clegg, S.L., 2021. Solid–liquid equilibria in aqueous solutions of Tris, Tris-NaCl, Tris-TrisHCl, and Tris-(TrisH)₂SO₄ at temperatures from 5 to 45 °C. *J. Chem. Eng. Data* 66 (437–455).
- Macaskill, J.B., Bates, R.G., 1975. Activity coefficients in aqueous mixtures of hydrochloric acid with “Tris” hydrochloride or t-butylammonium chloride at 25 °C. *J. Chem. Eng. Data* 20, 397–398.
- Macaskill, J.B., Bates, R.G., 1986. Osmotic and activity coefficients of TRIS-sulphate from isopiestic vapour pressure measurements at 25 °C. *J. Chem. Eng. Data* 31, 416–418.
- Millero, F.J., Roy, R.N., 1997. A chemical equilibrium model for the carbonate system in natural waters. *Croat. Chem. Acta* 70, 1–38.
- Millero, F.J., Hershey, J.P., Fernandez, M., 1987. The pK^{*} of TRIS⁺ in Na-K-Mg-Ca-Cl-SO₄ brines - pH scales. *Geochim. Cosmochim. Acta* 51, 707–711.
- Millero, F.J., Zhong, J.Z., Fiol, S., Sotolongo, S., Roy, R.N., Lee, K., Mane, S., 1993. The use of buffers to measure the pH of seawater. *Mar. Chem.* 44, 143–152.
- Millero, F.J., Graham, T.B., Huang, F., Bustos-Serrano, H., Pierrot, D., 2006. Dissociation constants of carbonic acid in seawater as a function of salinity and temperature. *Mar. Chem.* 100, 80–94.
- Mosley, L.M., Husheer, S.L.G., Hunter, K.A., 2004. Spectrophotometric pH measurement in estuaries using thymol blue and m-cresol purple. *Mar. Chem.* 91, 175–186.
- Müller, J.D., Rehder, G., 2018. Metrology of pH measurements in brackish waters—part 2: experimental characterization of purified meta-cresol purple for spectrophotometric pH_T measurements. *Front. Mar. Sci.* 5 (art. 177), 9 pp.
- Müller, J.D., Bastkowski, F., Sander, B., Seitz, S., Turner, D.R., Dickson, A.G., Rehder, G., 2018. Metrology for pH measurements in brackish waters—part 1: extending electrochemical pH_T measurements of TRIS buffers to salinities 5–20. *Front. Mar. Sci.* 5 (Art. 176), 12 pp.
- Orr, J.C., Epitalon, J.-M., Dickson, A.G., Gattuso, J.-P., 2018. Routine uncertainty propagation for the marine carbon dioxide system. *Mar. Chem.* 91, 84–107.
- Papadimitriou, S., Loucaides, S., Rérolle, V., Achterberg, E.P., Dickson, A.G., Mowlem, M., Kennedy, H., 2016. The measurement of pH in saline and hypersaline media at sub-zero temperatures: characterization of Tris buffers. *Mar. Chem.* 184, 11–20.
- Pierrot, D., Millero, F.J., 2016. The speciation of metals in natural waters. *Aquat. Geochem.* 23 (1), 1–20.
- Pitzer, K.S., 1991. Ion interaction approach: Theory and data correlation. In: Pitzer, K.S. (Ed.), *Activity Coefficients in Electrolyte Solutions*, 2nd edn. CRC Press, Boca Raton, pp. 75–153.
- Pitzer, K.S., 1995. *Thermodynamics*, 3rd edn. McGraw-Hill.
- Pratt, K.W., 2014. Measurement of pH_T values of Tris buffers in artificial seawater at varying mole ratios of Tris:Tris-HCl. *Mar. Chem.* 162, 89–95.
- Ramette, R.W., Culberson, C.H., Bates, R.G., 1977. Acid-base properties of Tris-(hydroxymethyl) amino methane (TRIS) buffers in seawater from 5 to 40 °C. *Anal. Chem.* 49, 867–870.
- Rard, J.A., Platford, R.F., 1991. Experimental methods: Isopiestic. In: Pitzer, K.S. (Ed.), *Activity Coefficients in Electrolyte Solutions*, 2nd edn. CRC Press, Boca Raton, pp. 209–277.
- Robinson, R.A., Bower, V.E., 1965. Osmotic and activity coefficients of tris (hydroxymethyl) aminomethane and its hydrochloride in aqueous solution at 25 °C. *J. Chem. Eng. Data* 10, 246–247.
- Tishchenko, P.Y., 2000. Non-ideal properties of the TRIS-TRIS.HCl-NaCl-H₂O buffer system in the 0–40 °C temperature interval. Application of the Pitzer equations. *Russ. Chem. Bull.* 49 (4), 674–679.
- Waters, J.F., Millero, F.J., 2013. The free proton concentration scale for seawater pH. *Mar. Chem.* 149, 8–22; and Waters, J.F., Millero, F.J., and Woosley, R.J., 2014, Corrigendum to “The free proton concentration scale for seawater pH”, *Mar. Chem.*, 165: 66–67.